Biomacromolecules

pubs.acs.org/Biomac

Article

# Toward a Complete Elucidation of the Primary Structure−Activity in Pentaerythritol-Based One-Component Ionizable Amphiphilic Janus Dendrimers for In Vivo Delivery of Luc-mRNA

Dipankar Sahoo,[§] Elena N. Atochina-Vasserman,[§] Juncheng Lu, Devendra S. Maurya, Nathan Ona, Jessica A. Vasserman, Houping Ni, Sydni Berkihiser, Wook-Jin Park, Drew Weissman,* and Virgil Percec*

Cite This: *Biomacromolecules* 2025, 26, 726−737

Read Online

ACCESS | Metrics & More | Article Recommendations | Supporting Information

**ABSTRACT:** Four-component lipid nanoparticles (LNPs) and viral vectors are key for mRNA vaccine and therapeutics delivery. LNPs contain ionizable lipids, phospholipids, cholesterol, and polyethylene glycol (PEG)-conjugated lipids and deliver mRNA for COVID-19 vaccines to liver when injected intravenously or intramuscularly. In 2021, we elaborated one-component ionizable amphiphilic Janus dendrimers (IAJDs) accessing targeted delivery of mRNA. Simplified synthesis and assembly processes allow for rapid IAJD screening for discovery. The role of the primary structure of IAJDs in activity indicated, with preliminary investigations, that ionizable amine (IA), sequence, and architecture of hydrophilic and hydrophobic domains are important for in vivo targeted delivery. Here, we study the role of the interconnecting linker length between the IA and the hydrophobic domain of pentaerythritol-based IAJDs. The linker length determines, through inductive effects, the position of the IA and the p$K_a$ of the IAJDs and through flexibility, the stability of the DNPs, highlighting their extraordinarily important role in effective targeted delivery.

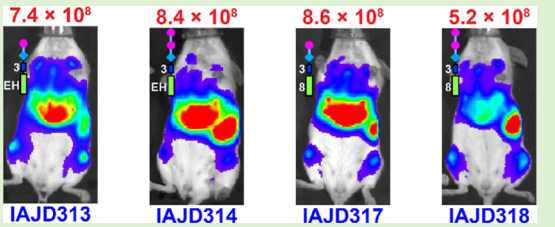


## INTRODUCTION

Viral and synthetic vectors facilitated the success of Covid-19 vaccines.[1−9] This achievement transformed the four-component lipid nanoparticles (LNPs) into the leading nonviral vectors for mRNA delivery to liver.[1−9] Viral and synthetic vectors exhibit advantages and disadvantages. The stable viral vectors show high transfection efficacy (95%)[10] and cell targeting.[11] LNPs are less stable[12] and less transfection efficient (1−2%).[13] However, viral vectors have drawbacks, including immunogenicity,[14] cytotoxicity,[15] difficult assembly,[16] inflammatory responses[12] to repeated administration, and insertional mutagenesis.[13] Advantages of LNPs include higher biosafety, lower toxicity, and immunogenicity,[13] with drawbacks such as the need for microfluidic or T-tube technology[17−20] for assembly, along with low-temperature for storage (−70 °C)[21] for stability in time. Some disadvantages of LNPs[22,23] arise from the unknown distribution of their 4-components within the LNP structure.[24,25] At neutral pH, ionizable amines (IA) segregate as an oil phase in the core of the LNPs, limiting transfection efficacy to 1−2%.[24,25] "PEG dilemma",[26−30] mediated by PEG-conjugated lipids, is another drawback. Permanently charged cationic lipids and dendrimers have pioneered DNA delivery[31−40] but are toxic and unsuitable to deliver less stable mRNA, which requires encapsulation to protect from enzymatic degradation.

During Covid-19 pandemic, our laboratories decided to eliminate some of the LNPs' weaknesses by incorporating all 4-component activities of LNPs into a single architecture named 1-component ionizable amphiphilic Janus dendrimer (IAJD),[41−48] and we accomplished targeted delivery, which requires 5-components with LNPs.[49,50] Amphiphilic JDs[51−73] and Janus glycodendrimers (JGDs)[74−81] were known to self-assemble into stable and monodisperse vesicles with predictable dimensions, known as dendrimersomes (DSs)[51−73] and glycodendrimersomes (GDSs).[74−81] This process is accomplished by simple injection of the JD or JGD ethanol solution into water or buffer, taking less than 1 min and requiring no special equipment. During the COVID-19 pandemic, the role of sequence and concentration of the carbohydrate part of the JGDs in the activity of their GDSs during agglutination to sugar-binding proteins was already elucidated.[74−81] This was accomplished using GDSs as models of the glycans in biological membranes. Therefore, replacing the carbohydrate part of the sequence-defined JGD with an IA

Received: November 14, 2024
Revised: December 9, 2024
Accepted: December 10, 2024
Published: December 17, 2024

**Scheme 1. Synthesis of Pentaerythritol (PE)-Based IAJDs with Different Linkers Interconnecting IAJDs to Hydrophobic Domains**

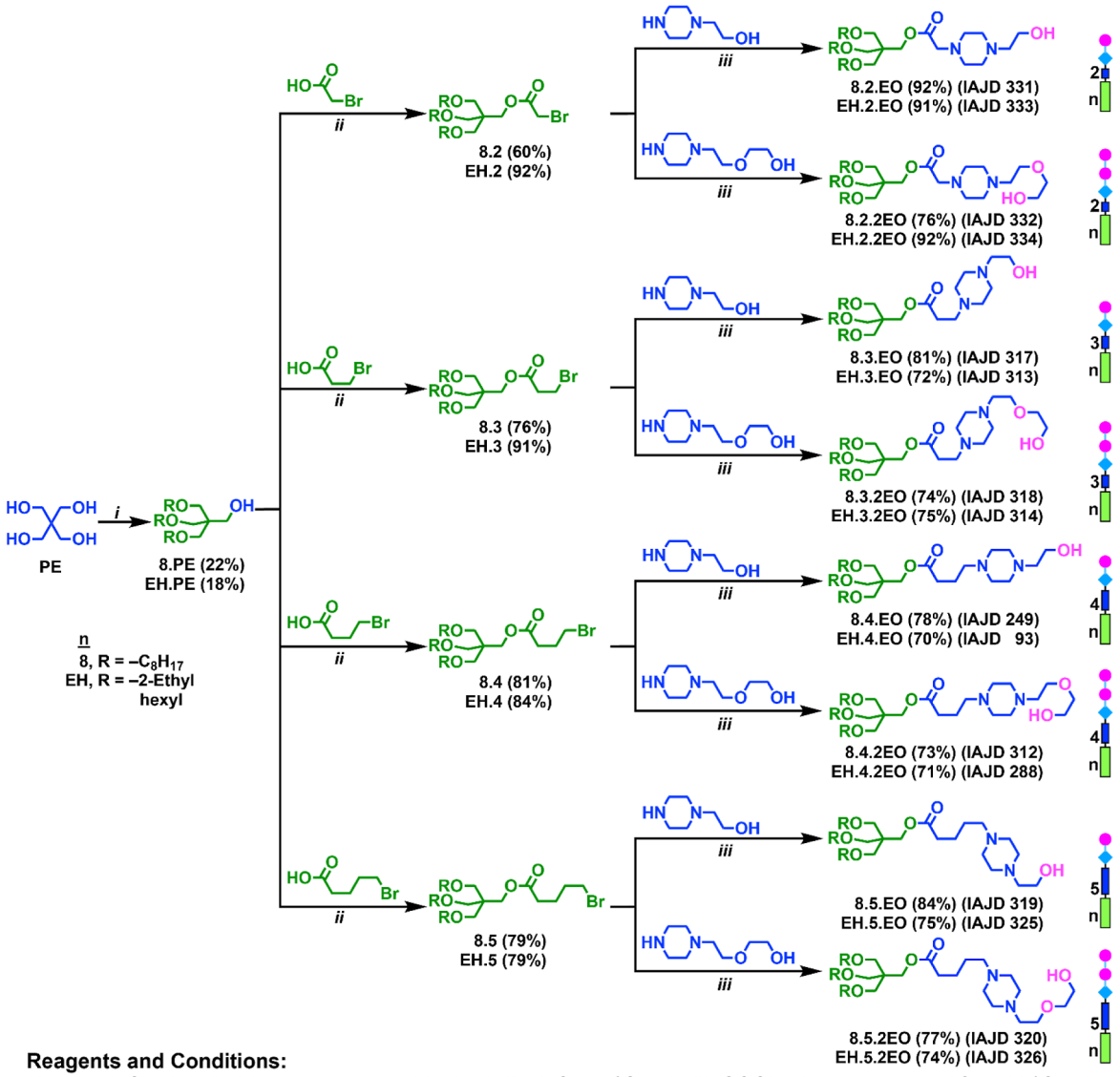


provided access to the first class of IAJDs.[41] Rapid screening of the primary structure, including architecture, p$K_a$ of IAs, sequence and structure of hydrophilic and hydrophobic domains of IAJD libraries obtained via modular-orthogonal methodologies, and coassembly of IAJDs with mRNA into DNPs, allowed for rapid discovery of molecular design principles for targeted delivery to the lung, liver, spleen, and lymph-nodes (LNs). One of the most active IAJDs reported is based on pentaerythritol (PE). This PE-based IAJD belongs to the simplified single−single (sSS) architecture, which is synthesized in only three reaction steps,[45] fewer than any other IAJD.[41−47] The role of the linker length interconnecting the IA to the hydrophobic fragment of IAJDs has never been investigated. Therefore, given the fact that PE-based IAJDs are made in just 3 steps, they became the target for the first series of investigations on the role of linker length interconnecting the IA to the hydrophobic domain of the IAJD. We hypothesized that the linker length must affect the p$K_a$ of the IAJD through inductive effects and the stability of the DNPs through its number of conformational isomers. While we could not predict the outcome of these investigations, we expected to uncover unexplored new principles, as has been the case in all previous studies on the role of the primary structure of the IAJD on in vivo luciferase activity. The preparation of a library of 12 sSS PE-based IAJDs to be discussed in this article is outlined in Scheme 1.

## EXPERIMENTAL SECTION

**Materials.** Pentaerythritol (Aldrich, 98%), tetrabutylammonium bromide (TBAB) (Acros Organics, 99%), 2-ethylhexyl bromide (Acros, Organics, 95%), 1-bromooctane (Aldrich, 99%), 3-bromopropanoic acid (Aldrich, 97%), 4-bromobutyric acid (Acros, 98%), 5-bromovaleric acid (TGI, 97%), 4-dimethylaminopyridine (DMAP) (TCI, 99%), *N*,*N*-dimethylformamide (Fisher Scientific), sodium hydroxide (Fisher Scientific), thionyl chloride (Aldrich, 99%), triethylamine (TCI, 99%), potassium carbonate (Fisher Scientific), 1-(2-hydroxyethyl)piperazine (Acros, 99%), and 1−2-(2-hydroxyethoxy)ethyl piperazine (TCI, 98%) were used as received. The decision for the selection of these two ionizable amines and of


https://doi.org/10.1021/acs.biomac.4c01599
Biomacromolecules 2025, 26, 726−737

the hydrophobic fragment will be discussed in a different publication. All other reagents and solvents, such as dichloromethane and acetonitrile, were sourced from commercial suppliers and used without further purification. Dichloromethane (DCM) and triethylamine ($NEt_3$) were dried over $CaH_2$ and were distilled under $N_2$ just before being used. A 10 mM acetate buffer was made by dissolving 2.3 mM sodium acetate and 7.7 mM acetic acid in ultrapure water. The final pH was rearranged using 0.1 M HCl or 0.1 M NaOH solution. Nucleoside-modified mRNA encoding firefly luciferase (Luc-mRNA) was synthesized as previously described.[82] DPBS (Corning), OptiMEM (Gibco), UltraPure DNase/RNase-Free Distilled Water (Invitrogen), Trypsin−EDTA (0.25%, Gibco), Trypan Blue (Sigma-Aldrich), Cell Culture Lysis 5× Reagent (Promega), Luciferase Assay System (Promega), and D-luciferin sodium salt (Regis Technologies) were used as received.

**Methods and Techniques.** The assessment of purity and structural characteristics of intermediates and end compounds was carried out using a range of analytical methods, which consists of a combination of thin-layer chromatography (TLC), proton and carbon nuclear magnetic resonance spectroscopy ($^1$H and $^{13}$C NMR), high-performance liquid chromatography (HPLC), and matrix-assisted laser desorption/ionization time-of-flight mass spectrometry (MALDI-TOF MS).

**$^1$H and $^{13}$C NMR.**[41−47] NMR spectra were recorded on a 400 MHz Bruker NEO NMR spectrometer with autosampling capability ($^1$H at 400 MHz, $^{13}$C at 101 MHz). Measurements were conducted at 23 °C using the solvent $CDCl_3$. Chemical shifts ($\delta$, ppm) with resonance multiplicities named singlet (s), doublet (d), triplet (t), multiplet (m), or broad resonance (br). Internal referencing was made with residual $CHCl_3$ from $CDCl_3$ ($^1$H: $\delta$ 7.26 ppm; $^{13}$C: $\delta$ 77.16 ppm) and tetramethylsilane (TMS: $\delta$, 0 ppm). Analysis was performed with MNova 14 software.

**Thin-Layer Chromatography.**[41−47] Reaction progress and compound purity were monitored using silica gel 60 $F_{254}$ TLC plates (E. Merck). Aromatic molecules were detected by UV light ($\lambda$ = 254 nm), while nonaromatic compounds were detected by staining with iodine vapors. Purification was achieved through flash column chromatography or column chromatography, employing silica gel (60 Å, 40−63 $\mu$m) from Silicycle and solvents specified in the experimental procedure for each compound.

**High-Pressure Liquid Chromatography.**[41−47] HPLC analysis was conducted to determine compound purity using a Shimadzu LC-20AD pump, a PE Nelson Analytical 900 Series integration station, a Shimadzu SPD-10A VP UV−vis detector ($\lambda$ = 254 nm), and a Shimadzu RID-10A refractive index (RI) detector. A setup of two AM gel columns (two 500 Å, 10 $\mu$m columns) was employed, with tetrahydrofuran (THF) containing 5% $NEt_3$ as the solvent at 23 °C. Compounds were identified using an RI detector.

**Matrix-Assisted Laser Desorption Ionization-Time of Flight Mass Spectrometry.**[41−47] Molecular masses were measured with a PerSeptive Biosystem Voyager-DE mass spectrometer (Framingham, MA) containing a nitrogen laser (337 nm) functioning in linear mode. Calibration was done with angiotensin II and bombesin standards. Samples for analysis were obtained by dissolving compounds in THF (5−10 mg/mL) and mixing with a matrix solution of 2,5-dihydroxybenzoic acid in THF (10 mg/mL) at a 1:5 ratio. After drying on a MALDI plate, samples were analyzed at 23 °C with instrument parameters tailored to the compound's molar mass.

**Dynamic Light Scattering.**[41−47] Particle size and polydispersities of DNPs were determined using a Malvern Zetasizer Nano S DLS machine with a 4 mW He−Ne laser (633 nm) and a photodiode at 175° to the beam. Measurements were performed at 23 °C in semimicro cuvettes (10 × 10 × 45 mm, Greiner Bio-One) containing an approximately 0.2 mL sample.

**p$K_a$ Measurements of Individual IAJDs.**[41−47] The p$K_a$ values of IAJDs were determined by the titration curve at the half-equivalence point. Solutions of IAJDs in ethanol saturated with NaCl (3 mL at 1.5 mg/mL) were incrementally titrated against 0.1 M HCl (increment of 7.5 mL), and the pH was determined with a Thermo Scientific Orion Star A121 m and Thermo Scientific Orion 8220BNWP pH probe.

**Production of Nucleoside-modified Luc-mRNA.** mRNA was synthesized as reported using T7 RNA polymerase on linearized DNA encoding codon-optimized Firefly Luciferase and a 101 nt poly(A) tail.[83] 1-Methylpseudouridine-5′-triphosphate was employed in place of UTP. A trinucleotide cap1 analogue was added cotranscriptionally. Purification followed previously reported procedures.[84] mRNA was analyzed for RNase, dsRNA, endotoxin, and other contaminants, then frozen and maintained at −20 °C.

**Formulation of DNPs Co-assembled from IAJDs and Luc-mRNA.**[41−47] A solution of nucleoside-modified mRNA encoding firefly luciferase (Luc-mRNA) in DNase/RNase-free distilled water was prepared at 4.0 mg/mL. IAJDs were dissolved in ethanol at 80 mg/mL. To prepare the mixture, 12.5 $\mu$L of the Luc-mRNA solution was placed into a clean, RNase-free 1.5 mL Eppendorf tube, followed by the addition of 463 $\mu$L of 10 mM acetate buffer (pH 4.0). Subsequently, 25 $\mu$L of the IAJD stock solution in ethanol was injected into the Luc-mRNA solution in acetate buffer, and the mixture was vortexed for 5 s. Rapid screening experiments demonstrated that bimodal distribution as well as polydispersity have no influence on in vivo activity. A quantitative discussion will be reported in an independent publication.

**In Vivo mRNA Delivery in Mice with DNPs.**[41−47] All mice used were handled in agreement with the guidelines and approval of the University of Pennsylvania Institutional Animal Care and Use Committee. Female BALB/c mice (6−8 weeks old, from Charles River Laboratories) were anesthetized with 3% isoflurane (Piramal Healthcare Limited) and injected via the retro-orbital sinus with 100 $\mu$L of DNP solution containing 10 $\mu$g of Luc-mRNA. After 4−6 h post injection, mice underwent luminescence characterization.

**Luminescence Characterization for In Vivo Transfection Experiments.**[41−47] Bioluminescence visualization was carried out using an IVIS Spectrum visualization system (PerkinElmer, Waltham, MA). Mice were anesthetized with 3% isoflurane (Piramal Healthcare Limited) and administered D-luciferin (Regis Technologies) intraperitoneally (i.p.) (150 mg/kg of body weight). Ten minutes after administering D-luciferin, the mice were placed on the imaging platform, maintained on isoflurane via a nose cone, and visualized at exposure times of 60, 30, or 15 s with medium binning (binning = 8) to ensure the signal was within the operative detection range. For imaging organs, the mice were sacrificed, and the heart, lungs, liver, and spleen were collected for bioluminescence visualization. Image analysis was performed using Living Image software (PerkinElmer), and bioluminescence values were determined by measuring photon flux (photons/second) in the region of interest.

**Molecular Modeling.**[44−46] Molecular models of the IAJDs were built using DS ViewerPro (version 5.0). Energy minimizations of the built models of the supramolecular structures were carried out with Material Studio (version 3.1) software from Accelrys. Display style and coloring were applied using BIOVIA Discovery Studio Visualizer (version 2019). The color codes used matched those in the ChemDraw structure: blue for the hydrophilic part, light and dark green for the hydrophobic part, pink for oxygen and OH groups, gray for carbons in the pentaerythritol core, light pink for the linker, and white for H groups on the aromatic ring.

**Synthesis.** *General Procedure for the Synthesis of PE-IAJDs with Two-, Three-, Four-, and Five-Carbon Linkers.* Synthesis of IAJDs involves the alkylation of PE under phase transfer catalyzed conditions[41−46,85−89] with *n*-octylbromide ($n$ = 8) and 2-ethylhexyl bromide (EH) in the presence of 50% NaOH at 80 °C for 5 h. Following the addition of water, the mixture containing tetra-alkylated, trialkylated, and dialkylated PE, along with the ether of the alkyl bromide, was extracted with DCM. The trialkyl compounds, ***n*.PE** (where $n$ = **8** and **EH**), were then isolated by column chromatography (silica gel, hexane/ethyl acetate 100/1 to 60/1) with yields of 22% and 18%, respectively.[45] Compounds ***n*.PE** were esterified with 2-bromoacetyl, 3-bromopropyl, 4-bromobutyl, and 5-bromopentyl chloride, which were produced in situ from the corresponding acids in dry DCM with $SOCl_2$ in the presence of


https://doi.org/10.1021/acs.biomac.4c01599
Biomacromolecules 2025, 26, 726−737

one drop of dry DMF for 1 h. This was followed by the distillation of DCM and excess $SOCl_2$ using a rotary evaporator. The esterification of ***n*.PE** with bromoalkyl chloride was carried out at 0−23 °C for 2 h in dry DCM with $NEt_3$ base and DMAP as a supernucleophilic catalyst.[90−92] This process generated compounds **n.2** to **n.5** with yields ranging from 60% to 92% after purification by column chromatography (silica gel, hexane/ethyl acetate 100/1 to 60/1). Compounds **n.2** to **n.5** were reacted with the ionizable amines *N*-(2-hydroxyethyl)piperazine, and *N*-(2-hydroxyethoxyethyl)piperazine in MeCN in the presence of $K_2CO_3$ for 3 h at 95 °C[41−44,89] to generate IAJDs 331, 333, 332, 334, 317, 313, 318, 314, 249, 93, 312, 288, 319, 325, 320, and 326 in isolated yields (after two purifications by column chromatography, silica gel, DCM/MeOH 50/1 to 20/1)[48] reported after their name in Scheme 1. The purity of all IAJDs, as determined by a combination of techniques, including TLC, $^1$HNMR, $^{13}$C NMR, HPLC, and MALDI-TOF, was over 99%. All IAJDs from Scheme 1 were coassembled with Luc-mRNA using the ethanol injection method into an acetate buffer containing Luc-mRNA (pH 4.0).[41−48]

*3-((2-Ethylhexyl)oxy)-2,2-bis(2-ethylhexyl)oxy)methyl)propan-1-ol (**EH.PE**).* Pentaerythritol (12.00 g, 88.1 mmol, 1 equiv) was added to a freshly made NaOH solution (140.8 g of NaOH and 120 mL of water), and the mixture was stirred for 1 h at 80 °C. 3-(Bromomethyl)heptane (51.07 g, 264.4 mmol, 3 equiv) and tetrabutylammonium bromide (TBAB) (3.55 g, 11.01 mmol, 0.125 equiv) were then added to the mixture, and heating was continued for 5 h. After 5 h, the reaction was halted and allowed to cool to room temperature. The resulting mixture was then diluted with 400 mL of water. The organic layer was extracted three times with 40 mL of DCM. The combined organic extracts were dried over anhydrous $MgSO_4$, filtered, and concentrated. The residue was purified by column chromatography ($SiO_2$) using hexane/ethyl acetate (100:1 to 60:1) as the eluent, yielding the title compound as a colorless oil (7.53 g, 18.1%). $^1$H NMR (400 MHz, $CDCl_3$): $\delta$ 3.71 (d, 2H, $CH_2$OH), 3.41(s, 6H, $-CH_2OCH_2CH(CH_2CH_3)(CH_2)_3CH_3$), 3.27 (d, 6H, $-CH_2OCH_2CH(CH_2CH_3)(CH_2)_3CH_3$), 3.14 (s, 1H, $CH_2OH$), 1.47 (m, 3H, $-CH_2OCH_2CH(CH_2CH_3)(CH_2)_3CH_3$), 1.40−1.20 (br, 24H, $-CH_2OCH_2CH(CH_2CH_3)(CH_2)_3CH_3$), 0.88 (m, 18H, $-CH_2OCH_2CH(CH_2CH_3)(CH_2)_3CH_3$). $^{13}$C NMR (101 MHz, $CDCl_3$): $\delta$ 74.4, 71.8, 70.0, 67.0, 45.0, 41.1, 39.7, 39.6, 39.1, 34.7, 34.5, 31.9, 31.6, 30.7, 29.1, 28.8, 25.3, 25.2, 24.0, 23.1, 22.8, 22.7, 20.7, 14.1, 14.1, 11.1.

*3-((2-Ethylhexyl)oxy)-2,2-bis(((2-ethylhexyl)oxy)methyl)propyl 2-Bromoacetate (**EH.2**).* 2-Bromoacetic acid (176 mg, 1.27 mmol, 2.0 equiv) was dissolved in 10 mL of dry DCM and 1 drop of DMF was added. $SOCl_2$ (91 mg, 0.762 mmol, 1.2 equiv) was added and the mixture was stirred at 23 °C for 1 h. Afterward, DCM and excess $SOCl_2$ were removed under reduced pressure, yielding 2-bromoacetyl chloride. Compound **EH.PE** (300 mg, 0.635 mmol, 1.0 equiv) and $NEt_3$ (77 mg, 0.762 mmol, 1.2 equiv) were dissolved in 10 mL anhydrous DCM. To this mixture were added the DCM solution (10 mL) and the above 2-bromoacetyl chloride dropwise at 0 °C. The mixture was allowed to warm to 23 °C with stirring for 2 h. Subsequently, 20 mL of water was added, and the mixture was extracted three times with 20 mL of DCM. The organic phase was collected, dried over anhydrous $MgSO_4$, and filtered. The filtrate was concentrated and purified by column chromatography ($SiO_2$) using hexane/ethyl acetate (40:1) as the eluent, yielding the title compound as a colorless oil (350 mg, 92%). $^1$H NMR (400 MHz, $CDCl_3$): $\delta$ 4.20 (s, 2H, $-CH_2COO$), 3.82 (s, 2H, $-OCOCH_2Br$), 3.36−3.24 (m, 12H, $-CH_2OCH_2(CH_2)_6CH_3$), 1.45 (m, 6H, $-OCH_2CH_2(CH_2)_5CH_3$), 1.28 (br, 30H, $-OCH_2CH_2(CH_2)_5CH_3$), 0.88 (m, 18H, $-OCH_2CH(CH_2CH_3)(CH_2CH_2CH_2CH_3)$). $^{13}$C NMR (101 MHz, $CDCl_3$): $\delta$ 166.9, 77.2, 74.2, 69.6, 69.5, 66.0, 44.9, 39.7, 30.7, 29.7, 29.1, 29.1, 24.0, 23.1, 14.1, 11.1.

*3-((2-Ethylhexyl)oxy)-2,2-bis(((2-ethylhexyl)oxy)methyl)propyl 3-Bromopropanoate (**EH.3**).* 3-Bromopropanoic acid (1.05 g, 6.87 mmol, 1.3 equiv) was dissolved in 15 mL of anhydrous DCM, and 1 drop of DMF was added. $SOCl_2$ (1.63 g, 13.75 mmol, 2.6 equiv) was added, and the mixture was stirred at 23 °C for 1 h. Afterward, DCM and excess $SOCl_2$ were removed under a vacuum to give the 3-bromopropanoyl chloride. Compound **EH.PE** (2.5 g, 5.29 mmol, 1.0 equiv), dry $NEt_3$ (0.69 g, 6.87 mmol, 1.3 equiv), and 4-dimethylaminopyridine (1.05 mg, 1.05 mmol, 0.2 equiv) were dissolved in 10 mL of anhydrous DCM. To this mixture was added the dry DCM solution (10 mL) of the above 3-bromopropanoyl chloride dropwise at 0 °C. The mixture was allowed to warm to 23 °C while stirring for 2 h. Subsequently, 20 mL of water was added, and the mixture was extracted three times with 20 mL of DCM. The organic phase was collected, dried over anhydrous $MgSO_4$, and filtered. The filtrate was then concentrated and purified by column chromatography ($SiO_2$) using hexane/ethyl acetate (40:1) as the eluent, yielding the title compound as a colorless oil (2.93 g, 91.2%). $^1$H NMR (400 MHz, $CDCl_3$): $\delta$ 4.12 (s, 2H, $-CH_2COO$), 3.45 (t, 2H, $-OCOCH_2CH_2CH_2Br$), 3.40−3.31 (m, 12H, $-CH_2OCH_2(CH_2)_4CH_3$), 2.48 (t, 2H, $-OCOCH_2CH_2CH_2Br$), 2.24−2.06 (m, 2H, $-CH_2OCOCH_2CH_2CH_2Br$), 1.54−1.46 (m, 12H, 3× $-OCH_2CH_2(CH_2)_3CH_3$), 1.28 (br, 18H, 3× $-OCH_2CH_2(CH_2)_3CH_3$), 0.90−0.84 (m, 9H, 3× $-O(CH_2)_5CH_3$). $^{13}$C NMR (101 MHz, $CDCl_3$): $\delta$ 172.3, 71.7, 69.6, 64.5, 53.5, 44.6, 32.8, 32.7, 31.8, 29.7, 28.0, 26.0, 22.8, 14.2.

*3-((2-Ethylhexyl)oxy)-2,2-bis(((2-ethylhexyl)oxy)methyl)propyl 4-Bromobutanoate (**EH.4**).* 4-Bromobutyric acid (0.96 g, 5.77 mmol, 1.3 equiv) was dissolved in 15 mL of dry DCM, and 1 drop of DMF was added. $SOCl_2$ (1.37 g, 11.54 mmol, 2.6 equiv) was added, and the mixture was stirred at 23 °C for 1 h. Afterward, DCM and excess $SOCl_2$ were removed under vacuum to give 4-bromopropanoyl chloride. Compound **EH.PE** (2.1 g, 4.44 mmol, 1.0 equiv), dry $NEt_3$ (584 mg, 5.77 mmol, 1.3 equiv), and 4-dimethylaminopyridine (108 mg, 0.8 mmol, 0.2 equiv) were dissolved in 10 mL of anhydrous DCM. To this mixture was added the dry DCM solution (10 mL) of the above 4-bromopropanoyl chloride dropwise at 0 °C. The mixture was allowed to warm to 23 °C with stirring during a 2 h period. Afterward, water (20 mL) was added, and the mixture was extracted three times with DCM (20 mL). The organic phase was collected, dried over anhydrous $MgSO_4$, and filtered. The filtrate was concentrated and purified by column chromatography ($SiO_2$) using hexane/ethyl acetate (40:1) as the eluent, yielding the title compound as a colorless oil (2.32 g, 84%). $^1$H NMR (400 MHz, $CDCl_3$): $\delta$ 4.09 (s, 2H, $-CH_2COO$), 3.45 (t, 2H, $-OCOCH_2CH_2CH_2Br$), 3.34 (s, 6H, $-CH_2OCH_2CH(CH_2CH_3)(CH_2)_3CH_3$), 3.23 (d, 6H, $-CH_2OCH_2CH(CH_2CH_3)(CH_2)_3CH_3$), 2.48 (t, 2H, $-OCOCH_2CH_2CH_2Br$), 2.16 (m, 2H, $-OCOCH_2CH_2CH_2Br$), 1.45 (m, 3H, $-CH_2OCH_2CH(CH_2CH_3)(CH_2)_3CH_3$), 1.39−1.14 (br, 24H, $-CH_2OCH_2CH(CH_2CH_3)(CH_2)_3CH_3$), 0.88 (m, 18H, $-CH_2OCH_2CH(CH_2CH_3)(CH_2)_3CH_3$). $^{13}$C NMR (101 MHz, $CDCl_3$): $\delta$ 174.5, 172.2, 74.2, 74.1, 69.8, 69.7, 69.3, 64.4, 64.2, 44.7, 44.6, 39.7, 32.7, 32.5, 31.6, 30.7, 29.2, 27.9, 24.0, 23.1, 22.7, 14.1, 11.1.

*3-((2-Ethylhexyl)oxy)-2,2-bis(((2-ethylhexyl)oxy)methyl)propyl 5-Bromopentanoate (**EH.5**).* 5-Bromovaleric acid (2.49 g, 13.7 mmol, 1.3 equiv) was dissolved in 15 mL of anhydrous DCM, and 1 drop of DMF was added. $SOCl_2$ (3.27 g, 27.5 mmol, 2.6 equiv) was added, and the mixture was stirred at 23 °C for 1 h. Afterward, DCM and excess $SOCl_2$ were removed under vacuum to give 5-bromovaleryl chloride. Compound **EH.PE** (5.0 g, 10.06 mmol, 1.0 equiv), dry $NEt_3$ (1.39 g, 13.7 mmol, 1.3 equiv), and 4-dimethylaminopyridine (258 mg, 2.1 mmol, 0.2 equiv) were dissolved in 10 mL of anhydrous DCM. To this mixture was added the dry DCM solution (10 mL) of the above 5-bromovaleryl chloride dropwise at 0 °C.

The mixture was allowed to warm to 23 °C while stirring for 2 h. Afterward, 20 mL of water was added, and the mixture was extracted three times with 20 mL of DCM. The combined organic phases were dried over anhydrous $MgSO_4$ and filtered. The filtrate was then concentrated and purified by column chromatography ($SiO_2$) using hexane/ethyl acetate (40:1) as the eluent, yielding the title compound as a colorless oil (5.3 g, 78.8%). $^1$H NMR (400 MHz, $CDCl_3$): $\delta$ 4.10 (s, 2H, $-CH_2COO$), 3.54 (t, 2H, $-OCOCH_2CH_2CH_2Br$), 3.25 (d, 6H, $-CH_2OCH_2CH(CH_2CH_3)-$), 2.53 (t, 2H, $-OCOCH_2CH_2CH_2Br$), 2.17 (m, 4H, $-CH_2OCOCH_2CH_2CH_2CH_2Br$), 1.51 (m, 6H, −


https://doi.org/10.1021/acs.biomac.4c01599
Biomacromolecules 2025, 26, 726−737

$OCH_2CH_2(CH_2)_5CH_3$), 1.45−1.41 (m, 3H, $CH_2OCH_2CH(CH_2CH_3)$−), 1.34−1.23 (br, 24H, $-OCH_2CH(CH_2CH_3)(CH_2CH_2CH_2CH_3)$), 0.91−0.85 (m, 18H, $-OCH_2CH(CH_2CH_3)(CH_2CH_2CH_2CH_3)$). $^{13}$C NMR (101 MHz, $CDCl_3$): δ 173.4, 71.8, 69.7, 64.3, 59.3, 57.8, 57.7, 53.2, 53.0, 44.6, 32.4, 32.0, 29.8, 29.8, 29.3, 26.3, 22.8, 22.3, 14.2.

*3-((2-Ethylhexyl)oxy)-2,2-bis(((2-ethylhexyl)oxy)methyl)propyl 2-(4-(2-hydroxyethyl)piperazin-1-yl)acetate (**EH.2.EO, IAJD 333**).* A mixture of compound **EH.2** (200 mg, 0.337 mmol, 1.0 equiv), 2-(piperazin-1-yl)ethan-1-ol (66 mg, 0.506 mmol, 1.5 equiv), $K_2CO_3$ (65 mg, 0.506 mmol, 1.5 equiv), and MeCN (10 mL) was heated to 95 °C and refluxed for 3 h.[89] After the mixture was cooled to 23 °C, the MeCN was removed under vacuum. Subsequently, 20 mL of water was added, and the mixture was extracted three times with 20 mL of DCM. The combined organic phases were dried over anhydrous $MgSO_4$ and filtered. The filtrate was concentrated to approximately 3 mL and purified by column chromatography ($SiO_2$) using DCM/MeOH (50:1 to 20:1) as the eluent. The purified product was then dried over anhydrous $MgSO_4$, and, after filtration and solvent evaporation, the title compound was obtained as a light-yellow oil (200 mg, 92%). $^1$H NMR (400 MHz, $CDCl_3$): δ 4.14 (s, 2H, $-CH_2OCO-$), 3.60 (t, 2H, $-NCH_2CH_2OH$), 3.33 (s, 6H, $-CH_2OCH_2CH(CH_2CH_3)-$), 3.26−3.16 (d, 8H, $-CH_2OCH_2CH(CH_2CH_3)-$ and $-COOCH_2$), 2.68−2.50 (br, 10H, $-N(CH_2CH_2)_2NCH_2CH_2OH$), 1.45 (m, 3H, $CH_2OCH_2CH(CH_2CH_3)-$), 1.38−1.16 (br, 24H, $-OCH_2CH(CH_2CH_3)(CH_2CH_2CH_2CH_3)$), 0.95−0.79 (m, 18H, $-OCH_2CH(CH_2CH_3)(CH_2CH_2CH_2CH_3)$). $^{13}$C NMR (101 MHz, $CDCl_3$): δ 170.1, 77.2, 74.2, 69.6, 64.4, 59.2, 59.1, 57.7, 52.9, 52.6, 44.7, 39.7, 30.7, 29.1, 24.0, 23.1, 14.1, 11.1. Purity by HPLC: 99+%. MALDI-TOF MS *m*/*z* of $[M + H]^+$ calcd for $C_{37}H_{75}N_2O_6$, 644.0; found, 645.0.

*3-((2-Ethylhexyl)oxy)-2,2-bis(((2-ethylhexyl)oxy)methyl)propyl 2-(4-(2-(2-Hydroxyethoxy)ethyl)piperazin-1-yl)acetate (**EH.2.2EO, IAJD 334**).* A mixture of compound **EH.2** (200 mg, 0.337 mmol, 1.0 equiv), 2-(2-(piperazin-1-yl)ethoxy)ethan-1-ol (88 mg, 0.506 mmol, 1.5 equiv), $K_2CO_3$ (65 mg, 0.506 mmol, 1.5 equiv), and MeCN (10 mL) was heated to 95 °C and refluxed for 3 h. The reaction mixture was then cooled to 23 °C, and the MeCN was removed under vacuum. Subsequently, 20 mL of water was added, and the mixture was extracted three times with 20 mL of DCM. The combined organic phases were dried over anhydrous $MgSO_4$ and filtered. The filtrate was concentrated to approximately 3 mL and purified by column chromatography ($SiO_2$) using DCM/MeOH (50:1 to 20:1) as the eluent. Finally, the product was dried over anhydrous $MgSO_4$, and, after filtration and solvent evaporation, the title compound was obtained as a light-yellow oil (210 mg, 91%). $^1$H NMR (400 MHz, $CDCl_3$): δ 4.13 (s, 2H, $-CH_2OCO-$), 3.75−3.55 (m, 6H, $-NCH_2CH_2OCH_2CH_2OH$), 3.32 (s, 6H, $-CH_2OCH_2CH(CH_2CH_3)-$), 3.27−3.11 (m, 8H, $-CH_2OCH_2CH(CH_2CH_3)-$ and $-COOCH_2$), 2.60 (br, 10H, $-N(CH_2CH_2)_2NCH_2CH_2OH$), 1.44 (m, 3H, $CH_2OCH_2CH(CH_2CH_3)-$) and $-COOCH_2CH_2CH_2CH_2$), 1.34−1.15 (br, 24H, $-OCH_2CH(CH_2CH_3)(CH_2CH_2CH_2CH_3)$), 0.93−0.75 (m, 18H, $-OCH_2CH(CH_2CH_3)(CH_2CH_2CH_2CH_3)$). $^{13}$C NMR (101 MHz, $CDCl_3$): δ 174.3, 77.2, 74.2, 72.4, 69.6, 67.4, 64.4, 62.1, 57.8, 53.0, 52.8, 44.7, 39.6, 30.7, 29.1, 24.0, 23.1, 14.1, 11.1. Purity by HPLC: 99+%. MALDI-TOF MS *m*/*z* of Purity by HPLC: 99+%. MALDI-TOF MS *m*/*z* of $[M + H]^+$ calcd for $C_{39}H_{79}N_2O_7$, 687.6; found, 688.7; $[M + Na]^+$ calculated for $C_{39}H_{78}N_2O_7Na$, 709.6; found, 710.3.

*3-(Pentadecyloxy)-2,2-bis((pentadecyloxy)methyl)propan-1-ol (**8.PE**).* Pentaerythritol (12.00 g, 88.1 mmol, 1 equiv) was added to a freshly made NaOH solution (140.8 g NaOH and 120 mL water), and the mixture was stirred for 1 h at 80 °C. 1-Bromooctane (51.07 g, 264.4 mmol, 3 equiv) and tetrabutylammonium bromide (TBAB) (3.55 g, 11.01 mmol, 0.125 equiv) were then added to the mixture, and heating was continued for 5 h. After 5 h, the reaction was halted and allowed to cool to room temperature. The resultant mixture was diluted with 400 mL of water and extracted three times with 40 mL of DCM. The combined organic phases were dried over anhydrous $MgSO_4$ and filtered. The filtrate was concentrated and purified by column chromatography ($SiO_2$) using hexane/ethyl acetate (100:1 to 60:1) as the eluent, yielding the title compound as a colorless oil (9.14 g, 21.9%). $^1$H NMR (400 MHz, $CDCl_3$): δ 3.70 (d, 2H, $CH_2OH$), 3.43 (s, 6H, $-CH_2OCH_2(CH_2)_6CH_3$), 3.38 (t, 6H, $-CH_2OCH_2(CH_2)_6CH_3$), 3.14(br, 1H, $CH_2OH$), 1.63−1.45 (m, 6H, $-OCH_2CH_2(CH_2)_5CH_3$), 1.28 (br, 30H, $-OCH_2CH_2(CH_2)_5CH_3$), 0.88 (m, 9H, $-O(CH_2)_7CH_3$). $^{13}$C NMR (101 MHz, $CDCl_3$): δ 71.8, 71.5, 66.7, 44.7, 31.9, 31.6, 29.6, 29.4, 29.3, 26.2, 22.7, 14.1.

*3-(Octyloxy)-2,2-bis((octyloxy)methyl)propyl 2-Bromoacetate (**8.2**).* 2-Bromoacetic acid (177 mg, 1.27 mmol, 1.2 equiv) was dissolved in 10 mL of dry DCM, and 1 drop of DMF was added. After that, $SOCl_2$ (252 mg, 2.12 mmol, 2 equiv) was then added to the mixture and allowed to stir at 23 °C for 1 h. Afterward, DCM and excess $SOCl_2$ were removed under vacuum to give the 5-bromovaleric chloride. Compound **8.PE** (500 mg, 1.06 mmol, 1.0 equiv) and dry $NEt_3$ (177 mg, 1.27 mmol, 1.2 equiv) were dissolved in 10 mL anhydrous DCM. To this mixture was added the dry DCM solution (10 mL) of the above 2-bromoacetic chloride dropwise at 0 °C. The mixture was stirred and allowed to warm to 23 °C over 2 h. Then, 20 mL of water was added, and the mixture was extracted three times with 20 mL of DCM. The combined organic phases were dried over anhydrous $MgSO_4$ and filtered. The filtrate was then concentrated and purified by column chromatography ($SiO_2$) using hexane/ethyl acetate (40:1) as the eluent), yielding the title compound as a colorless oil (380 mg, 60%). $^1$H NMR (400 MHz, $CDCl_3$): δ 4.24 (s, 2H, $-CH_2COO$), 4.04 (s, 2H, $-OCOOCH_2Br$), 3.44−3.26 (m, 12H, $-CH_2OCH_2(CH_2)_6CH_3$), 1.51 (m, 6H, $-OCH_2CH_2(CH_2)_5CH_3$), 1.29 (br, 30H, $-OCH_2CH_2(CH_2)_5CH_3$), 0.88 (m, 9H, $-O(CH_2)_7CH_3$). $^{13}$C NMR (101 MHz, $CDCl_3$): δ 167.1, 77.2, 71.6, 69.4, 69.3, 66.0, 44.6, 41.0, 31.9, 29.6, 29.5, 29.3, 26.2, 22.7, 14.1.

*3-(Octyloxy)-2,2-bis((octyloxy)methyl)propyl 3-Bromopropanoate (**8.3**).* 3-Bromopropanoic acid (2.10 g, 13.7 mmol, 1.3 equiv) was dissolved in 15 mL of dry DCM and 1 drop of DMF was added. $SOCl_2$ (1.99 g, 27.5 mmol, 2.6 equiv) was added and the mixture was stirred at 23 °C for 1 h. Afterward, DCM and excess $SOCl_2$ were removed under reduced pressure to give 3-bromopropanoyl chloride. Compound **8.PE** (5.0 g, 10.5 mmol, 1.0 equiv), dry $NEt_3$ (1.39 g, 13.7 mmol, 1.3 equiv), and 4-dimethylaminopyridine (0.258 g, 2.1 mmol, 0.2 equiv) were dissolved in 10 mL of dry DCM. To this mixture was added the dry DCM solution (10 mL) of the above 3-bromopropanoyl chloride dropwise at 0 °C. The mixture was stirred and allowed to warm to 23 °C over 2 h. Subsequently, 20 mL of water was added, and the mixture was extracted three times with 20 mL of DCM. The combined organic phases were dried over anhydrous $MgSO_4$ and filtered. The filtrate was concentrated and purified by column chromatography ($SiO_2$) using hexane/ethyl acetate (40:1) as the eluent, yielding the title compound as a colorless oil (4.9 g, 76.2%). $^1$H NMR (400 MHz, $CDCl_3$): δ 4.12 (s, 2H, $-CH_2COO$), 3.43 (t, 2H, $-OCOCH_2CH_2CH_2Br$), 3.38−3.30 (m, 12H, $-CH_2OCH_2(CH_2)_6CH_3$), 2.37−2.31 (m, 2H, $-CH_2OCOCH_2CH_2CH_2Br$), 1.67−1.57 (m, 2H, $-CH_2OCOCH_2CH_2CH_2Br$), 1.51 (m, 6H, $-OCH_2CH_2(CH_2)_5CH_3$), 1.29 (br, 30H, $-OCH_2CH_2(CH_2)_5CH_3$), 0.89 (m, 9H, $-O(CH_2)_7CH_3$). $^{13}$C NMR (101 MHz, $CDCl_3$): δ 173.0, 77.4, 71.7, 68.5, 68.5, 64.5, 44.5, 32.5, 32.5, 31.9, 29.5, 29.4, 29.5, 28.0, 26.1, 22.5, 14.0.

*3-(Octyloxy)-2,2-bis((octyloxy)methyl)propyl 4-Bromobutanoate (**8.4**).* 4-Bromobutyric acid (2.29 g, 13.74 mmol, 1.3 equiv) was dissolved in 15 mL of dry DCM, and 1 drop of DMF was added. $SOCl_2$ (3.27 g, 27.48 mmol, 2.6 equiv) was added and the vacuum to give the 4-bromopropanoyl chloride. Compound **8.PE** (5.0 g, 10.5 mmol, 1.0 equiv), dry $NEt_3$ (1.39 g, 13.74 mmol, 1.0 equiv), and 4-dimethylaminopyridine (258 mg, 2.1 mmol, 0.2 equiv) were dissolved in 10 mL of dry DCM. To this mixture were added the dry DCM solution (10 mL) and the above 4-bromopropanoyl chloride dropwise at 0 °C. The mixture was stirred and allowed to warm to 23 °C over a 2 h period. Afterward, 20 mL of water was added, and the mixture was extracted three times with 20 mL of DCM. The combined organic


https://doi.org/10.1021/acs.biomac.4c01599
Biomacromolecules 2025, 26, 726−737

phases were dried over anhydrous $MgSO_4$ and filtered. The filtrate was then concentrated and purified by column chromatography ($SiO_2$) using hexane/ethyl acetate (40:1) as the eluent, yielding the title compound as a colorless oil (5.3 g, 80.6%). $^1$H NMR (400 MHz, $CDCl_3$) $\delta$ 4.13 (s, 2H, $-CH_2COO$), 3.46 (t, 2H, $-OCOCH_2CH_2CH_2Br$), 3.39−3.31 (m, 12H, $-CH_2OCH_2(CH_2)_6CH_3$), 2.49 (t, 2H, $-OCOCH_2CH_2CH_2Br$), 2.18 (m, 2H, $-CH_2OCOCH_2CH_2CH_2Br$), 1.51 (m, 6H, $-OCH_2CH_2(CH_2)_5CH_3$), 1.29 (br, 30H, $-OCH_2CH_2(CH_2)_5CH_3$), 0.88 (m, 9H, $-O(CH_2)_7CH_3$). $^{13}$C NMR (101 MHz, $CDCl_3$): $\delta$ 172.3, 77.2, 71.6, 69.5, 69.5, 64.4, 44.4, 32.7, 32.6, 31.9, 29.6, 29.5, 29.3, 27.9, 26.2, 22.7, 14.1.

*3-(Octyloxy)-2,2-bis((octyloxy)methyl)propyl 5-Bromopentanoate (**8.5**).* 5-Bromovaleric acid (2.74 g, 13.75 mmol, 1.3 equiv) was dissolved in 15 mL of dry DCM, and 1 drop of DMF was added. $SOCl_2$ (3.27 g, 27.5 mmol, 2.6 equiv) was added, and the mixture was stirred at 23 °C for 1 h. Afterward, DCM and excess $SOCl_2$ were removed under vacuum to give the 5-bromovaleric chloride. Compound **8.PE** (5.0 g, 10.57 mmol, 1.0 equiv), dry $NEt_3$ (1.39 g, 13.75 mmol, 1.3 equiv), and 4-dimethylaminopyridine (0.258 g, 2.1 mmol, 0.2 equiv) were dissolved in 10 mL of dry DCM. To this mixture were added the dry DCM solution (10 mL) and the above 5-bromovaleric chloride dropwise at 0 °C. The mixture was stirred and allowed to warm to 23 °C over a 2 h duration. Subsequently, 20 mL of water was added, and the mixture was extracted three times with 20 mL of DCM. The combined organic phases were dried over anhydrous $MgSO_4$ and filtered. The filtrate was then concentrated and purified by column chromatography ($SiO_2$) using hexane/ethyl acetate (40:1) as the eluent, yielding the title compound as a colorless oil (5.3 g, 78.8%). $^1$H NMR (400 MHz, $CDCl_3$) $\delta$ 4.15 (s, 2H, $-CH_2COO$), 3.53 (t, 2H, $-OCOCH_2CH_2CH_2Br$), 3.39−3.33 (m, 12H, $-CH_2OCH_2(CH_2)_6CH_3$), 2.47 (t, 2H, $-OCOCH_2CH_2CH_2Br$), 2.18 (m, 4H, $-CH_2OCOCH_2CH_2CH_2CH_2Br$), 1.53 (m, 6H, $-OCH_2CH_2(CH_2)_5CH_3$), 1.30 (br, 30H, $-OCH_2CH_2(CH_2)_5CH_3$), 0.89 (m, 9H, $-O(CH_2)_7CH_3$). $^{13}$C NMR (101 MHz, $CDCl_3$): $\delta$ 173.7, 71.7, 69.3, 64.1, 59.0, 57.3, 57.2, 53.1, 53.0, 45.0, 32.1, 32.3, 29.7, 29.7, 29.7, 26.1, 22.5, 22.1, 14.0.

*3-(Octyloxy)-2,2-bis((octyloxy)methyl)propyl 2-(4-(2-Hydroxyethyl)piperazin-1-yl) Acetate (**8.2.EO, IAJD 331**).* A mixture of compound **8.2** (500 mg, 0.84 mmol, 1.0 equiv), 2-(piperazin-1-yl)ethan-1-ol (131 mg, 1.01 mmol, 1.2 equiv), $K_2CO_3$ (139 mg, 1.01 mmol, 1.2 equiv), and MeCN (15 mL) was heated to 95 °C and refluxed for 3 h.[89] The reaction mixture was cooled to 23 °C, and the MeCN was removed under vacuum. Subsequently, 20 mL of water was added, and the mixture was extracted three times with 20 mL of DCM. The combined organic phases were dried over anhydrous $MgSO_4$ and filtered. The filtrate was concentrated to approximately 3 mL and purified by column chromatography ($SiO_2$) using DCM/MeOH (50:1 to 20:1) as the eluent. The product was dried over anhydrous $MgSO_4$, and, after filtration and solvent evaporation, the title compound was obtained as a light-yellow oil (500 mg, 92%). $^1$H NMR (400 MHz, $CDCl_3$): $\delta$ 4.16 (s, 2H, $-CH_2OCO-$), 3.61 (t, 2H, $-NCH_2CH_2OH$), 3.39−3.30 (m, 12H, $-CH_2OCH_2(CH_2)_6CH_3$), 3.21 (s, 2H, $-COOCH_2-$), 2.70−2.51 (br, 10H, $-N(CH_2CH_2)_2NCH_2CH_2OH$); 1.561 (m, 6H, $-OCH_2CH_2(CH_2)_5CH_3$), 1.37−1.19 (br, 30H, $-OCH_2CH_2(CH_2)_5CH_3$), 0.92−0.81 (m, 9H, $-O(CH_2)_7CH_3$). $^{13}$C NMR (101 MHz, $CDCl_3$): $\delta$ 170.1, 77.2, 71.6, 69.5, 64.4, 59.2, 59.2, 57.6, 52.9, 52.6, 44.5, 31.9, 29.6, 29.5, 29.3, 26.2, 22.7, 14.1. Purity by HPLC: 99+%. MALDI-TOF MS $m/z$ of $[M + H]^+$ calcd for $C_{37}H_{75}N_2O_6$, 643.6; found, 643.0.

*3-(Octyloxy)-2,2-bis((octyloxy)methyl)propyl 2-(4-(2-(2-Hydroxyethoxy)ethyl)piperazin-1-yl)acetate (**8.2.EO, IAJD 332**).* A mixture of compound **8.2** (630 mg, 1.06 mmol, 1 equiv), 2-(2-(piperazin-1-yl)ethoxy)ethan-1-ol (221 mg, 1.27 mmol, 1.2 equiv), $K_2CO_3$ (176 mg, 1.27 mmol, 1.2 equiv), and MeCN (15 mL) was heated to 95 °C and refluxed for 3 h.[89] The reaction mixture was cooled to 23 °C, and MeCN was removed under reduced pressure. Subsequently, 20 mL of water was added, and the mixture was extracted three times with 20 mL of DCM. The combined organic phases were dried over anhydrous $MgSO_4$ and filtered. The filtrate was concentrated to approximately 3 mL and purified by column chromatography ($SiO_2$) using DCM/MeOH (50:1 to 20:1) as the eluent. The product was then dried over anhydrous $MgSO_4$. Finally, filtration and evaporation of the solvent yielded the title compound as a light-yellow oil (550 mg, 76%). $^1$H NMR (400 MHz, $CDCl_3$): $\delta$ 4.15 (s, 2H, $-CH_2OCO-$), 3.71−3.58 (m, 6H, $-NCH_2CH_2OCH_2CH_2OH$), 3.40−3.28 (m, 12H, $-CH_2OCH_2(CH_2)_6CH_3$), 3.18 (s, 2H, $-COOCH_2-$), 2.60 (br, 10H, $-N(CH_2CH_2)_2NCH_2CH_2O-$), 1.50 (m, 6H, $-OCH_2CH_2(CH_2)_5CH_3$), 1.27 (br, 30H, $-OCH_2CH_2(CH_2)_5CH_3$), 0.93−0.76 (m, 9H, $-O(CH_2)_7CH_3$). $^{13}$C NMR (101 MHz, $CDCl_3$): $\delta$ 170.1, 77.2, 72.4, 71.6, 69.4, 67.4, 64.3, 62.1, 59.2, 57.8, 53.0, 52.8, 44.5, 31.9, 29.6, 29.5, 29.3, 26.2, 22.7, 14.1. Purity by HPLC: 99+%. MALDI-TOF MS $m/z$ of $[M + H]^+$ calcd for $C_{39}H_{79}N_2O_7$, 687.6; found, 687.5.

*3-(Octyloxy)-2,2-bis((octyloxy)methyl)propyl 2-(4-(2-Hydroxyethyl)piperazin-1-yl)acetate (**8.2.EO, IAJD 331**).* A mixture of compound **8.2** (500 mg, 0.84 mmol, 1.0 equiv), 2-(piperazin-1-yl)ethan-1-ol (131 mg, 1.01 mmol, 1.2 equiv), $K_2CO_3$ (139 mg, 1.01 mmol, 1.2 equiv), and MeCN (15 mL) was heated to 95 °C and refluxed for 3 h.[89] After the reaction mixture was cooled to 23 °C, the MeCN was removed under reduced pressure. The resulting mixture was then extracted three times with 20 mL of DCM after addition of 20 mL of water. The combined organic phases were dried over anhydrous $MgSO_4$ and filtered. The filtrate was concentrated to approximately 3 mL and purified by column chromatography ($SiO_2$) using DCM/MeOH (50:1 to 20:1) as the eluent. The product was dried over anhydrous $MgSO_4$. Finally, filtration and evaporation of the solvent yielded the title compound as a light-yellow oil (500 mg, 92%). $^1$H NMR (400 MHz, $CDCl_3$): $\delta$ 4.16 (s, 2H, $-CH_2OCO-$), 3.61 (t, 2H, $-NCH_2CH_2OH$), 3.39−3.30 (m, 12H, $-CH_2OCH_2(CH_2)_6CH_3$), 3.21 (s, 2H, $-COOCH_2-$), 2.70−2.51 (br, 10H, $-N(CH_2CH_2)_2NCH_2CH_2OH$); 1.561 (m, 6H, $-OCH_2CH_2(CH_2)_5CH_3$), 1.37−1.19 (br, 30H, $-OCH_2CH_2(CH_2)_5CH_3$), 0.92−0.81 (m, 9H, $-O(CH_2)_7CH_3$). $^{13}$C NMR (101 MHz, $CDCl_3$): $\delta$ 170.1, 77.2, 71.6, 69.5, 64.4, 59.2, 59.2, 57.6, 52.9, 52.6, 44.5, 31.9, 29.6, 29.5, 29.3, 26.2, 22.7, 14.1. Purity by HPLC: 99+%. MALDI-TOF MS $m/z$ of $[M + H]^+$ calcd for $C_{37}H_{75}N_2O_6$, 643.6; found, 643.0.

*3-(Octyloxy)-2,2-bis((octyloxy)methyl)propyl 2-(4-(2-(2-Hydroxyethoxy)ethyl)piperazin-1-yl)acetate (**8.2.EO, IAJD 332**).* A mixture of compound **8.2** (630 mg, 1.06 mmol, 1 equiv), 2-(2-(piperazin-1-yl)ethoxy)ethan-1-ol (221 mg, 1.27 mmol, 1.2 equiv), $K_2CO_3$ (176 mg, 1.27 mmol, 1.2 equiv), and MeCN (15 mL) was heated to 95 °C and refluxed for 3 h.[89] The reaction mixture was cooled to 23 °C, and the MeCN was removed under reduced pressure. Then, 20 mL of water was added, and the mixture was extracted three times with 20 mL of DCM. The combined organic phases were dried over anhydrous $MgSO_4$ and filtered. The filtrate was concentrated to approximately 3 mL and purified by column chromatography ($SiO_2$) using DCM/MeOH (50:1 to 20:1) as the eluent. The product was further dried over anhydrous $MgSO_4$. Filtration and evaporation of the solvent yielded the title compound as a light-yellow oil (550 mg, 76%). $^1$H NMR (400 MHz, $CDCl_3$): $\delta$ 4.15 (s, 2H, $-CH_2OCO-$), 3.71−3.58 (m, 6H, $-NCH_2CH_2OCH_2CH_2OH$), 3.40−3.28 (m, 12H, $-CH_2OCH_2(CH_2)_6CH_3$), 3.18 (s, 2H, $-COOCH_2-$), 2.60 (br, 10H, $-N(CH_2CH_2)_2NCH_2CH_2O-$), 1.50 (m, 6H, $-OCH_2CH_2(CH_2)_5CH_3$), 1.27 (br, 30H, $-OCH_2CH_2(CH_2)_5CH_3$), 0.93−0.76 (m, 9H, $-O(CH_2)_7CH_3$). $^{13}$C NMR (101 MHz, $CDCl_3$): $\delta$ 170.1, 77.2, 72.4, 71.6, 69.4, 67.4, 64.3, 62.1, 59.2, 57.8, 53.0, 52.8, 44.5, 31.9, 29.6, 29.5, 29.3, 26.2, 22.7, 14.1. Purity by HPLC: 99+%. MALDI-TOF MS $m/z$ of $[M + H]^+$ calcd for $C_{39}H_{79}N_2O_7$, 687.6; found, 687.5.

## RESULTS AND DISCUSSION

Both IAJDs and LNPs are not toxic, and additional details on this issue will be reported in a different publication. Figure 1



https://doi.org/10.1021/acs.biomac.4c01599
Biomacromolecules 2025, 26, 726−737

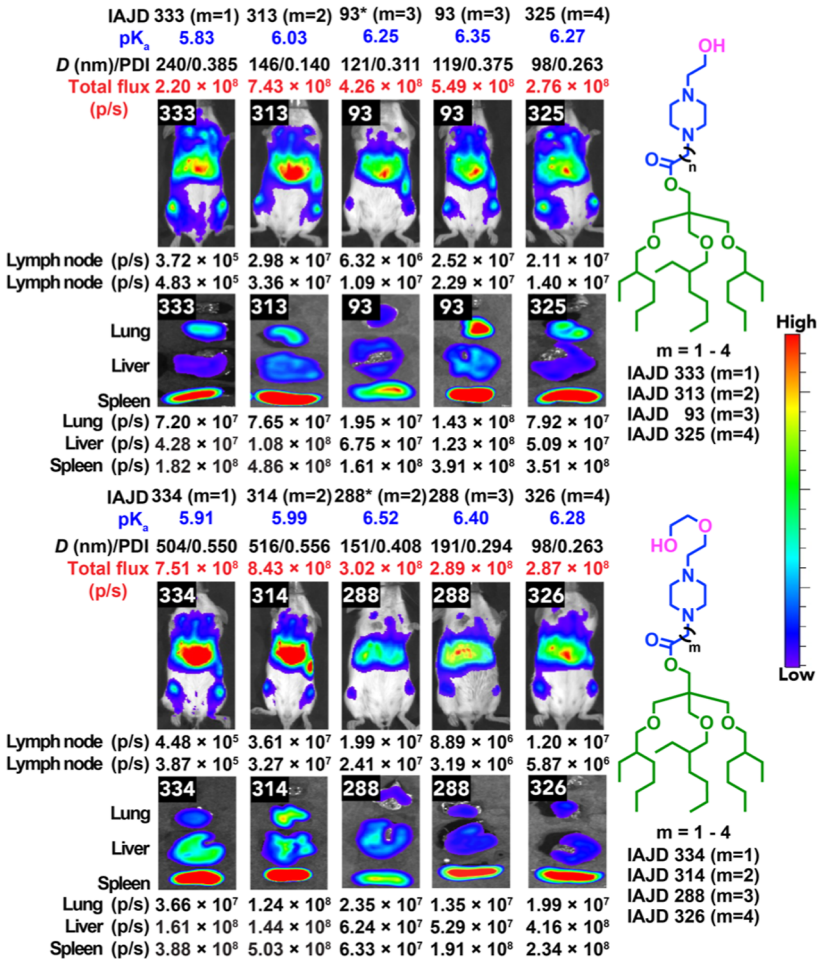


**Figure 1.** Comparison of representative in vivo images of luciferase activities of EH-based PE IAJDs with two-, three-, four-, and five-carbon linkers. The results marked with an asterisk (*) are from previously published data.[45]

presents the data for the eight ethylhexyl substituted PE-based IAJDs and the delivery of Luc-mRNA with their DNPs. p$K_a$ values of the IAJDs are in blue on the first row after the IAJD numbers. Dimensions and polydispersities of the resulting DNPs, determined by DLS, are summarized on second row in black, followed by total flux (in p/s) in red. Delivery to lymph nodes values are provided alongside the overall image of the mice, while values for targeted delivery to lung, liver, and spleen organs are shown beneath the individual images of the corresponding organs.

The first observation is that p$K_a$ values of IAJDs are determined by linker length. Two- and three-carbon linker IAJDs, have the lowest p$K_a$ values followed by four- and five-carbon linker IAJDs respectively. This demonstrates the inductive effect of the linker on the p$K_a$ of IA attached to it. The two-carbon linker contains an electron-withdrawing ester carbonyl at the second carbon, which inductively increases the positive charge on the protonated nitrogen from piperazine, thereby decreasing its p$K_a$. A smaller effect is seen for the three-carbon linker. A reverse effect is observed with four- and five-carbon linkers. In these cases, the electron-withdrawing character of the ester carbonyl is dominated by the electron-donating character of the longer alkyl group, which stabilizes the positive charge on the protonated nitrogen attached to it and thus increases the p$K_a$. The lowest p$K_a$ in this case may occur for the nitrogen attached to the hydroxyethyl group(s). The second significant effect of the linker length, derived from the number of conformers, is visibly apparent. The longer linker containing five-carbons provides the most fluid IAJDs, while the three-carbon linker generates the most viscous IAJDs. A lower p$K_a$ and less flexible three-carbon linker favor deprotonation and increased stability of DNPs, while longer-linkers have the opposite effect. The two-carbon linker has the lowest p$K_a$ and only one favorable conformer, while longer-linkers have more conformers (Figures S42 and S43). Therefore, longer linkers provide better bilayer stability. The optimum combination of p$K_a$ and bilayer stability was detected for the linker containing 3 carbons. However, additional research required to elucidate this complex combination is in progress, and it will be reported soon.

We will now discuss the role of the linker-length on the total and targeted in vivo delivery of Luc-mRNA. At least three in vivo experiments were performed after the coassembly of IAJDs with Luc-mRNA, without optimization for dimensions and polydispersities. Whole body luciferase activities for IAJD 313, IAJD314, and IAJD334 containing a three-carbon and two-carbon linkers were $7.43 \times 10^8$, $8.43 \times 10^8$, and $7.51 \times 10^8$ p/s respectively. These luciferase values are up to three times higher than the corresponding values for IAJD93 and IAJD288, containing four- and two-carbon linkers, and about three times higher than for IAJDs 325 and 326, which are based on five-carbon linkers and for two-carbon linker IAJD333. Luciferase activities in the spleen are also up to two times higher when comparing IAJDs 314 and 334 with 288 newly synthesized


https://doi.org/10.1021/acs.biomac.4c01599
Biomacromolecules 2025, 26, 726−737

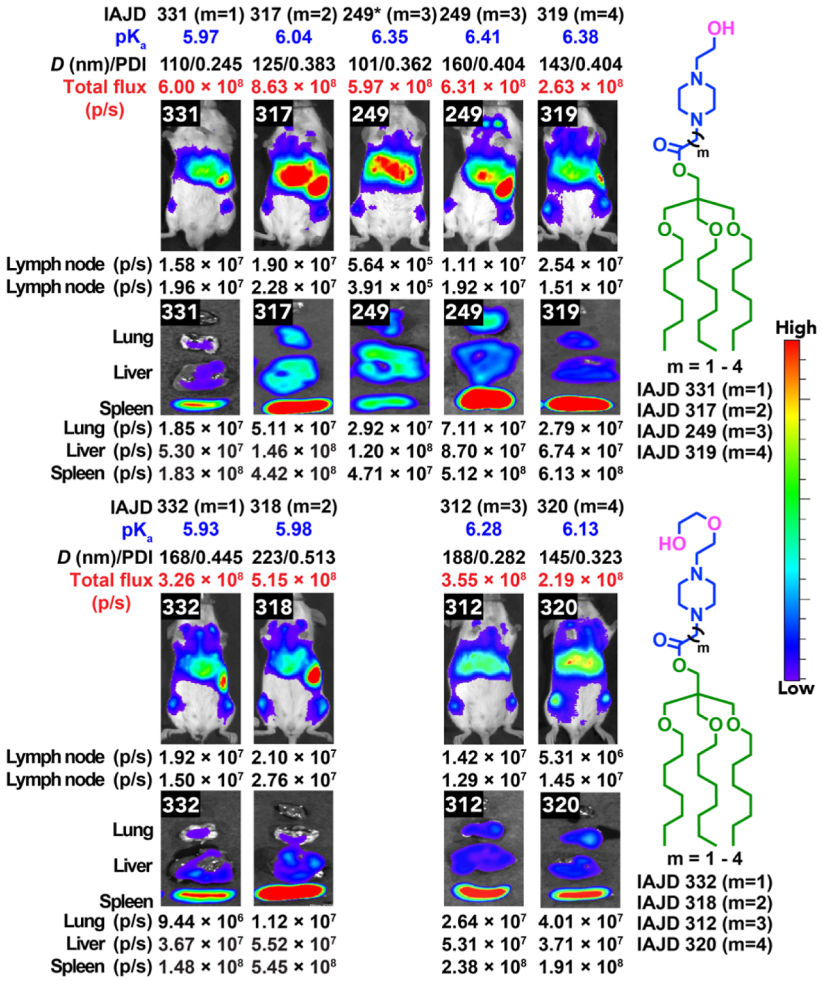


**Figure 2.** Comparison of in vivo images of luciferase activities of n-octyl-based pentaerythritol IAJDs with two-, three-, four-, and five-carbon linkers. The results marked with an asterisk (*) are from previously published data.[45]

ones and IAJD333 containing three-, two-, and four-carbon linkers, respectively. There is a general trend indicating higher whole body or organ-specific luciferase activities for IAJDs with three- and two-carbon linkers. The lowest activities are consistent for five-carbon linkers.

Figure 2 summarizes the results for PE-based IAJDs containing *n*-octyl in their hydrophobic part. A similar p$K_a$ trend was observed. It is important to note that the ethylhexyl-based IAJDs from Figure 1 are constitutional isomers of the *n*-octyl-based IAJDs from Figure 2. Therefore, while their activities are expected to be different,[44] trends in p$K_a$ and in vivo experiment values must be similar. IAJDs 317, 331, and 318 containing three- and two-carbon linkers show the highest whole body luciferase flux activities of $8.63 \times 10^8$, $6.00 \times 10^8$, and $5.15 \times 10^8$ p/s, respectively. The whole-body luciferase activity of approximately $9 \times 10^8$ p/s for IAJD 317 is the highest obtained so far for the delivery of Luc-mRNA mediated with DNPs based on IAJDs. As with the results from Figure 1, total luciferase flux activities of IAJDs 317 and 318 containing three-carbon linkers are 1.5 to 3.3 times higher than those of the corresponding IAJDs 249 and 312 containing four-carbon linkers as well as IAJDs 319 and 320 with five-carbon linkers and of IAJDs 331 and 332 with two carbon-linkers. A similar trend was observed for luciferase activities in the spleen. In all cases, IAJDs with three-carbon linkers are more active than those with four- or five- and even two-carbon linkers by a factor of about 1.4 when comparing IAJD 317 and IAJD 249 and by a factor of about 3.3 to 3.9 for the other IAJDs.

Figure 3 combines all results of the entire library of 16 IAJDs from Figures 1 and 2, including data not shown in these figures along with their statistical analysis. Figure 3 contains both unpublished and published data. The published data are marked with an asterisk (*) and refer to IAJD codes 93, 288, and 249. As shown in Figures 1 and 2, these IAJDs were also resynthesized, and their data were compared with the results obtained from the new samples. When inspecting Figure 3, we proceeded from left to right. To aid in the visualization of these data, we compare both IAJD numbers with their schematic cartoon representations, as shown in Scheme 1. The first set of data is for IAJD 333, which contains a two-carbon linker, compared with IAJDs 313, 93*, and 93, which have three- and four-carbon linkers, and IAJD 325, which has a five-carbon linker. The three-carbon linker IAJD313 has the highest activity, and this trend repeats for all sublibraries summarized in Figure 3.

## CONCLUSIONS

In conclusion, the maximum luciferase activity was observed for all three-carbon linker IAJDs 313, 314, 317, and 318 in all four sublibraries investigated. The linker length decides the p$K_a$ of the IA, but also at least for the case discussed here, it also determines the number of its conformers, which most probably


https://doi.org/10.1021/acs.biomac.4c01599
Biomacromolecules 2025, 26, 726−737

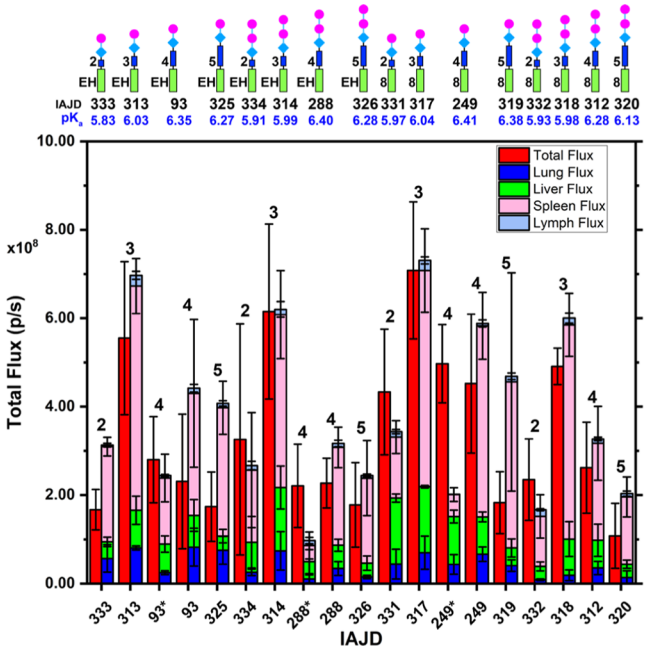


**Figure 3.** Comparison of in vivo luciferase activity of pentaerythritol IAJDs with different linker lengths. Results marked with an asterisk (*) are from previous published data.[45]

provides a cooperative and synergistic effect[93] on the delivery of mRNA. This trend was unexpected and could not have been predicted before performing these in vivo experiments. This tendency highlights the extraordinarily important role of the linker length in interconnecting the IA to the hydrophobic domain of the IAJDs. Depending on the balance between the inductive effects of the linker and the hydroxyethyl substituents, the protonated nitrogen from piperazine most probably changes position, with p$K_a$ and DNP stability determining in vivo activity. We expect that the linker length concept reported here is general for all IA-based mRNA delivery systems including IAJDs and 4-component LNPs. We also expect that different steric restrictions interconnecting the linker to the hydrophobic part provide access to different in vivo activities for the linker providing the lowest p$K_a$ values. The results reported here have demonstrated that a complete elucidation of primary structure−activity in all systems for the delivery of mRNA must involve the primary structure of the hydrophilic domain, the structure of the ionizable amine, the primary structure of the hydrophobic part, and the linker interconnecting the hydrophilic to the hydrophobic fragments, including in more recently developed IAJDs.[94] More experiments along this line with different libraries of IAJDs to elucidate completely the primary structure−activity dependence for IAJDs are in progress and will be reported soon.

## ■ ASSOCIATED CONTENT

### Supporting Information

The Supporting Information is available free of charge at https://pubs.acs.org/doi/10.1021/acs.biomac.4c01599.

Experimental methods, synthesis and characterization of IAJDs and their analytical data, their DNPs with mRNA, in vitro and in vivo data of all DNPs, DLS curves of DNPs, stability characterization of DNPs, p$K_a$ measurements, molecular models, and supplemental references (PDF)

## ■ AUTHOR INFORMATION


### Corresponding Authors

**Drew Weissman** − *Department of Medicine, Perelman School of Medicine, University of Pennsylvania, Philadelphia, Pennsylvania 19104, United States;* orcid.org/0000-0002-1501-6510; Email: dreww@pennmedicine.upenn.edu

**Virgil Percec** − *Roy & Diana Vagelos Laboratories, Department of Chemistry, University of Pennsylvania, Philadelphia, Pennsylvania 19104-6323, United States;* orcid.org/0000-0001-5926-0489; Email: percec@sas.upenn.edu

### Authors

**Dipankar Sahoo** − *Roy & Diana Vagelos Laboratories, Department of Chemistry, University of Pennsylvania, Philadelphia, Pennsylvania 19104-6323, United States;* orcid.org/0000-0002-7646-6419

**Elena N. Atochina-Vasserman** − *Department of Medicine, Perelman School of Medicine, University of Pennsylvania, Philadelphia, Pennsylvania 19104, United States;* orcid.org/0000-0001-7950-7004

**Juncheng Lu** − *Roy & Diana Vagelos Laboratories, Department of Chemistry, University of Pennsylvania, Philadelphia, Pennsylvania 19104-6323, United States*

**Devendra S. Maurya** − *Roy & Diana Vagelos Laboratories, Department of Chemistry, University of Pennsylvania, Philadelphia, Pennsylvania 19104-6323, United States;* orcid.org/0000-0002-4488-9927

**Nathan Ona** − *Department of Medicine, Perelman School of Medicine, University of Pennsylvania, Philadelphia, Pennsylvania 19104, United States;* orcid.org/0000-0002-8729-2223

**Jessica A. Vasserman** − *Department of Medicine, Perelman School of Medicine, University of Pennsylvania, Philadelphia, Pennsylvania 19104, United States*

**Houping Ni** − *Department of Medicine, Perelman School of Medicine, University of Pennsylvania, Philadelphia, Pennsylvania 19104, United States*

**Sydni Berkihiser** − *Department of Medicine, Perelman School of Medicine, University of Pennsylvania, Philadelphia, Pennsylvania 19104, United States*

**Wook-Jin Park** − *Department of Medicine, Perelman School of Medicine, University of Pennsylvania, Philadelphia, Pennsylvania 19104, United States*

Complete contact information is available at: https://pubs.acs.org/10.1021/acs.biomac.4c01599


### Author Contributions

[§]D.S. and E.N.A.-V. contributed equally to this work.

### Notes

The authors declare no competing financial interest.

## ■ ACKNOWLEDGMENTS

This work was supported by National Science Foundation Grants DMR-2104554 and DMR-1720530, the P. Roy Vagelos Chair at the University of Pennsylvania, and the Alexander von Humboldt Foundation (all to V.P.). NMR Instrumentation (NEO400) was supported by the NSF Major Research Instrumentation Program (award NSF CHE-1827457) and Vagelos Institute for Energy Science and Technology.

## REFERENCES


(1) Whitehead, K. A.; Langer, R.; Anderson, D. G. Knocking down Barriers: Advances in SiRNA Delivery. *Nat. Rev. Drug Discovery* **2009**, *8*, 129−138.

(2) Cullis, P. R.; Hope, M. J. Lipid Nanoparticle Systems for Enabling Gene Therapies. *Mol. Ther.* **2017**, *25*, 1467−1475.

(3) Buschmann, M. D.; Carrasco, M. J.; Alishetty, S.; Paige, M.; Alameh, M. G.; Weissman, D. Nanomaterial Delivery Systems for mRNA Vaccines. *Vaccines* **2021**, *9*, 65.

(4) Wilson, J. M. Genetic Diseases, Immunology, Viruses, and Gene Therapy. *Hum. Gene Ther.* **2014**, *25*, 257−261.

(5) Nguyen, J.; Szoka, F. C. Nucleic Acid Delivery: The Missing Pieces of the Puzzle? *Acc. Chem. Res.* **2012**, *45*, 1153−1162.

(6) Lacroix, A.; Sleiman, H. F. DNA Nanostructures: Current Challenges and Opportunities for Cellular Delivery. *ACS Nano* **2021**, *15*, 3631−3645.

(7) Billingsley, M. M.; Singh, N.; Ravikumar, P.; Zhang, R.; June, C. H.; Mitchell, M. J. Ionizable Lipid Nanoparticle-Mediated mRNA Delivery for Human CAR T Cell Engineering. *Nano Lett.* **2020**, *20*, 1578−1589.

(8) Huang, X.; Kong, N.; Zhang, X.; Cao, Y.; Langer, R.; Tao, W. The Landscape of mRNA Nanomedicine. *Nat. Med.* **2022**, *28*, 2273−2287.

(9) Yin, H.; Kanasty, R. L.; Eltoukhy, A. A.; Vegas, A. J.; Dorkin, J. R.; Anderson, D. G. Non-Viral Vectors for Gene-Based Therapy. *Nat. Rev. Genet.* **2014**, *15*, 541−555.

(10) Luo, D.; Saltzman, W. M. Synthetic DNA Delivery Systems. *Nat. Biotechnol.* **2000**, *18*, 33−37.

(11) Wickham, T. J. Ligand-Directed Targeting of Genes to the Site of Disease. *Nat. Med.* **2003**, *9*, 135−139.

(12) Hajj, K. A.; Whitehead, K. A. Tools for Translation: Non-Viral Materials for Therapeutic mRNA Delivery. *Nat. Rev. Mater.* **2017**, *2*, 1−17.

(13) Ramamoorth, M.; Narvekar, A. Non Viral Vectors in Gene Therapy- an Overview. *J. Clin. Diagn. Res.* **2015**, *9*, GE01-06.

(14) Baum, C.; Kustikova, O.; Modlich, U.; Li, Z.; Fehse, B. Mutagenesis and Oncogenesis by Chromosomal Insertion of Gene Transfer Vectors. *Hum. Gene Ther.* **2006**, *17*, 253−263.

(15) Bessis, N.; GarciaCozar, F. J.; Boissier, M.-C. Immune Responses to Gene Therapy Vectors: Influence on Vector Function and Effector Mechanisms. *Gene Ther.* **2004**, *11*, S10−S17.

(16) Bouard, D.; Alazard-Dany, D.; Cosset, F.-L. Viral Vectors: From Virology to Transgene Expression. *Br. J. Pharmacol.* **2009**, *157*, 153−165.

(17) Chen, D.; Love, K. T.; Chen, Y.; Eltoukhy, A. A.; Kastrup, C.; Sahay, G.; Jeon, A.; Dong, Y.; Whitehead, K. A.; Anderson, D. G. Rapid Discovery of Potent Sirna-Containing Lipid Nanoparticles Enabled by Controlled Microfluidic Formulation. *J. Am. Chem. Soc.* **2012**, *134*, 6948−6951.

(18) Zhigaltsev, I. V.; Belliveau, N.; Hafez, I.; Leung, A. K.; Huft, J.; Hansen, C.; Cullis, P. R. Bottom-up Design and Synthesis of Limit Size Lipid Nanoparticle Systems with Aqueous and Triglyceride Cores Using Millisecond Microfluidic Mixing. *Langmuir* **2012**, *28*, 3633−3640.

(19) Leung, A. K.; Hafez, I. M.; Baoukina, S.; Belliveau, N. M.; Zhigaltsev, I. V.; Afshinmanesh, E.; Tieleman, D. P.; Hansen, C. L.; Hope, M. J.; Cullis, P. R. Lipid Nanoparticles Containing Sirna Synthesized by Microfluidic Mixing Exhibit an Electron-Dense Nanostructured Core. *J. Phys. Chem. C* **2012**, *116*, 18440−18450.

(20) Leung, A. K.; Tam, Y. Y.; Chen, S.; Hafez, I. M.; Cullis, P. R. Microfluidic Mixing: A General Method for Encapsulating Macromolecules in Lipid Nanoparticle Systems. *J. Phys. Chem. B* **2015**, *119*, 8698−8706.

(21) Pardi, N.; Hogan, M. J.; Porter, F. W.; Weissman, D. mRNA Vaccines — a New Era in Vaccinology. *Nat. Rev. Drug Discovery* **2018**, *17*, 261−279.

(22) Jayaraman, M.; Ansell, S. M.; Mui, B. L.; Tam, Y. K.; Chen, J.; Du, X.; Butler, D.; Eltepu, L.; Matsuda, S.; Narayanannair, J. K.; Rajeev, K. G.; Hafez, I. M.; Akinc, A.; Maier, M. A.; Tracy, M. A.; Cullis, P. R.; Madden, T. D.; Manoharan, M.; Hope, M. J. Maximizing the Potency of siRNA Lipid Nanoparticles for Hepatic Gene Silencing In Vivo. *Angew. Chem., Int. Ed.* **2012**, *51*, 8529−8533.

(23) Kulkarni, J. A.; Witzigmann, D.; Chen, S.; Cullis, P. R.; van der Meel, R. Lipid Nanoparticle Technology for Clinical Translation of siRNA Therapeutics. *Acc. Chem. Res.* **2019**, *52*, 2435−2444.

(24) Ramezanpour, M.; Schmidt, M. L.; Bodnariuc, I.; Kulkarni, J. A.; Leung, S. S. W.; Cullis, P. R.; Thewalt, J. L.; Tieleman, D. P. Ionizable Amino Lipid Interactions with POPC: Implications for Lipid Nanoparticle Function. *Nanoscale* **2019**, *11*, 14141−14146.

(25) Kulkarni, J. A.; Darjuan, M. M.; Mercer, J. E.; Chen, S.; van der Meel, R.; Thewalt, J. L.; Tam, Y. Y. C.; Cullis, P. R. On the Formation and Morphology of Lipid Nanoparticles Containing Ionizable Cationic Lipids and siRNA. *ACS Nano* **2018**, *12*, 4787−4795.

(26) Hatakeyama, H.; Akita, H.; Harashima, H. A Multifunctional Envelope Type Nano Device (MEND) for Gene Delivery to Tumours Based on the EPR Effect: A Strategy for Overcoming the PEG Dilemma. *Adv. Drug Delivery Rev.* **2011**, *63*, 152−160.

(27) Sato, Y.; Hatakeyama, H.; Sakurai, Y.; Hyodo, M.; Akita, H.; Harashima, H. A pH-Sensitive Cationic Lipid Facilitates the Delivery of Liposomal siRNA and Gene Silencing Activity in Vitro and in Vivo. *J. Controlled Release* **2012**, *163*, 267−276.

(28) Choi, J. S.; MacKay, J. A.; Szoka, F. C. Low-pH-Sensitive PEG-Stabilized Plasmid−Lipid Nanoparticles: Preparation and Characterization. *Bioconjugate Chem.* **2003**, *14*, 420−429.

(29) Pelegri-O'Day, E. M.; Lin, E.-W.; Maynard, H. D. Therapeutic Protein−Polymer Conjugates: Advancing Beyond PEGylation. *J. Am. Chem. Soc.* **2014**, *136*, 14323−14332.

(30) Whitfield, C. J.; Zhang, M.; Winterwerber, P.; Wu, Y.; Ng, D. Y. W.; Weil, T. Functional DNA−Polymer Conjugates. *Chem. Rev.* **2021**, *121*, 11030−11084.

(31) Kukowska-Latallo, J. F.; Bielinska, A. U.; Johnson, J.; Spindler, R.; Tomalia, D. A.; Baker, J. R. Efficient Transfer of Genetic Material into Mammalian Cells Using Starburst Polyamidoamine Dendrimers. *Proc. Natl. Acad. Sci. U.S.A.* **1996**, *93*, 4897−4902.

(32) Zhou, J.; Wu, J.; Hafdi, N.; Behr, J.-P.; Erbacher, P.; Peng, L. PAMAM Dendrimers for Efficient SiRNA Delivery and Potent Gene Silencing. *Chem. Commun.* **2006**, No. 22, 2362.

(33) Posadas, I.; Guerra, F.; Cena, V. Nonviral Vectors for the Delivery of Small Interfering RNAs to the CNS. *Nanomed* **2010**, *5*, 1219−1236.

(34) Rodrigo, A. C.; Rivilla, I.; Perez-Martinez, F. C.; Monteagudo, S.; Ocana, V.; Guerra, J.; Garcia-Martinez, J. C.; Merino, S.; Sanchez-Verdu, P.; Cena, V.; Rodríguez-López, J. Efficient, Non-Toxic Hybrid PPV-PAMAM Dendrimer as a Gene Carrier for Neuronal Cells. *Biomacromolecules* **2011**, *12*, 1205−1213.

(35) Majoral, J.-P.; Caminade, A. M. Dendrimers Containing Heteroatoms (Si, P, B, Ge, or Bi). *Chem. Rev.* **1999**, *99*, 845−880.

(36) Janiszewska, J.; Posadas, I.; Jativa, P.; Bugaj-Zarebska, M.; Urbanczyk-Lipkowska, Z.; Cena, V. Second Generation Amphiphilic Poly-Lysine Dendrons Inhibit Glioblastoma Cell Proliferation without Toxicity for Neurons or Astrocytes. *PLoS One* **2016**, *11*, No. e0165704.

(37) Haensler, J.; Szoka, F. C. Polyamidoamine Cascade Polymers Mediate Efficient Transfection of Cells in Culture. *Bioconjugate Chem.* **1993**, *4*, 372−379.

(38) Loup, C.; Zanta, M.-A.; Caminade, A.-M.; Majoral, J.-P.; Meunier, B. Preparation of Water-Soluble Cationic Phosphorus-Containing Dendrimers as DNA Transfecting Agents. *Chem.—Eur. J.* **1999**, *5*, 3644−3650.

(39) Pedziwiatr-Werbicka, E.; Chonco, L.; Shcharbin, D.; de Jesus, E.; Bermejo, J. F.; Ortega, P.; de la Mata, F. J.; Flores, J. C.; Gomez, R.; Klajnert, B.; Munoz-Fernandez, M. A.; Bryszewska, M. Carbosilane Dendrimers as Drug Carriers. *Eur. J. Clin. Invest.* **2007**, *37*, 79.

(40) Zinselmeyer, B. H.; Mackay, S. P.; Schatzlein, A. G.; Uchegbu, I. F. The Lower-Generation Polypropylenimine Dendrimers Are Effective Gene-Transfer Agents. *Pharm. Res.* **2002**, *19*, 960−967.




https://doi.org/10.1021/acs.biomac.4c01599
*Biomacromolecules* 2025, 26, 726−737

(41) Zhang, D.; Atochina-Vasserman, E. N.; Maurya, D. S.; Huang, N.; Xiao, Q.; Ona, N.; Liu, M.; Shahnawaz, H.; Ni, H.; Kim, K.; Billingsley, M. M.; Pochan, D. J.; Mitchell, M. J.; Weissman, D.; Percec, V. One-Component Multifunctional Sequence-Defined Ionizable Amphiphilic Janus Dendrimer Delivery Systems for mRNA. *J. Am. Chem. Soc.* **2021**, *143*, 12315−12327.
(42) Zhang, D.; Atochina-Vasserman, E. N.; Maurya, D. S.; Liu, M.; Xiao, Q.; Lu, J.; Lauri, G.; Ona, N.; Reagan, E. K.; Ni, H.; Weissman, D.; Percec, V. Targeted Delivery of MRNA with One-Component Ionizable Amphiphilic Janus Dendrimers. *J. Am. Chem. Soc.* **2021**, *143*, 17975−17982.
(43) Zhang, D.; Atochina-Vasserman, E. N.; Lu, J.; Maurya, D. S.; Xiao, Q.; Liu, M.; Adamson, J.; Ona, N.; Reagan, E. K.; Ni, H.; Weissman, D.; Percec, V. The Unexpected Importance of the Primary Structure of the Hydrophobic Part of One-Component Ionizable Amphiphilic Janus Dendrimers in Targeted MRNA Delivery Activity. *J. Am. Chem. Soc.* **2022**, *144*, 4746−4753.
(44) Lu, J.; Atochina-Vasserman, E. N.; Maurya, D. S.; Shalihin, M. I.; Zhang, D.; Chenna, S. S.; Adamson, J.; Liu, M.; Shah, H. U. R.; Shah, H.; Xiao, Q.; Queeley, B.; Ona, N. A.; Reagan, E. K.; Ni, H.; Sahoo, D.; Peterca, M.; Weissman, D.; Percec, V. Screening Libraries to Discover Molecular Design Principles for the Targeted Delivery of mRNA with One-Component Ionizable Amphiphilic Janus Dendrimers Derived from Plant Phenolic Acids. *Pharmaceutics* **2023**, *15*, 1572.
(45) Lu, J.; Atochina-Vasserman, E. N.; Maurya, D. S.; Sahoo, D.; Ona, N.; Reagan, E. K.; Ni, H.; Weissman, D.; Percec, V. Targeted and Equally Distributed Delivery of mRNA to Organs with Pentaerythritol-Based One-Component Ionizable Amphiphilic Janus Dendrimers. *J. Am. Chem. Soc.* **2023**, *145* (34), 18760−18766.
(46) Sahoo, D.; Atochina-Vasserman, E. N.; Maurya, D. S.; Arshad, M.; Chenna, S. S.; Ona, N.; Vasserman, J. A.; Ni, H.; Weissman, D.; Percec, V. The Constitutional Isomerism of One-Component Ionizable Amphiphilic Janus Dendrimers Orchestrates the Total and Targeted Activities of mRNA Delivery. *J. Am. Chem. Soc.* **2024**, *146* (6), 3627−3634.
(47) Zhang, D.; Xiao, Q. W.; Rahimzadeh, M.; Liu, M.; Rodriguez-Emmenegger, C.; Miyazaki, Y.; Shinoda, W.; Percec, V. Self-Assembly of Glycerol-Amphiphilic Dendrimers Amplifies and Indicates Principles for the Selection of Stereochemistry by Biological Membranes. *J. Am. Chem. Soc.* **2023**, *145*, 4311−4323.
(48) Arshad, M.; Atochina-Vasserman, E. N.; Chenna, S. S.; Maurya, D. S.; Shalihin, M. I.; Sahoo, D.; Lewis, A. C.; Lewis, J. J.; Ona, N.; Vasserman, J. A.; Ni, H.; Park, W.-J.; Weissman, D.; Percec, V. Accelerated Ten-Gram-Scale Synthesis of One-Component Multifunctional Sequence-Defined Ionizable Amphiphilic Janus Dendrimer 97. *Biomacromolecules* **2024**, *25*, 6871−6882.
(49) Cheng, Q.; Wei, T.; Farbiak, L.; Johnson, L. T.; Dilliard, S. A.; Siegwart, D. J. Selective Organ Targeting (SORT) Nanoparticles for Tissue-Specific mRNA Delivery and CRISPR-Cas Gene Editing. *Nat. Nanotechnol.* **2020**, *15*, 313−320.
(50) Han, X.; Alameh, M.-G.; Butowska, K.; Knox, J. J.; Lundgreen, K.; Ghattas, M.; Gong, N.; Xue, L.; Xu, Y.; Lavertu, M.; Bates, P.; Xu, J.; Nie, G.; Zhong, Y.; Weissman, D.; Mitchell, M. J. Adjuvant Lipidoid-Substituted Lipid Nanoparticles Augment the Immunogenicity of SARS-CoV-2 MRNA Vaccines. *Nat. Nanotechnol.* **2023**, *18*, 1105.
(51) Percec, V.; Wilson, D. A.; Leowanawat, P.; Wilson, C. J.; Hughes, A. D.; Kaucher, M. S.; Hammer, D. A.; Levine, D. H.; Kim, A. J.; Bates, F. S.; Davis, K. P.; Lodge, T. P.; Klein, M. L.; DeVane, R. H.; Aqad, E.; Rosen, B. M.; Argintaru, A. O.; Sienkowska, M. J.; Rissanen, K.; Nummelin, S.; et al. Self-Assembly of Janus Dendrimers into Uniform Dendrimersomes and Other Complex Architectures. *Science* **2010**, *328*, 1009−1014.
(52) Sherman, S. E.; Xiao, Q.; Percec, V. Mimicking Complex Biological Membranes and Their Programmable Glycan Ligands with Dendrimersomes and Glycodendrimersomes. *Chem. Rev.* **2017**, *117*, 6538−6631.
(53) Peterca, M.; Percec, V.; Leowanawat, P.; Bertin, A. Predicting the Size and Properties of Dendrimersomes from the Lamellar Structure of Their Amphiphilic Janus Dendrimers. *J. Am. Chem. Soc.* **2011**, *133*, 20507−20520.
(54) Zhang, S.; Sun, H.-J.; Hughes, A. D.; Draghici, B.; Lejnieks, J.; Leowanawat, P.; Bertin, A.; Otero De Leon, L.; Kulikov, O. V.; Chen, Y.; Pochan, D. J.; Heiney, P. A.; Percec, V. Single−Single" Amphiphilic Janus Dendrimers Self-Assemble into Uniform Dendrimersomes with Predictable Size. *ACS Nano* **2014**, *8*, 1554−1565.
(55) Zhang, S.; Sun, H.-J.; Hughes, A. D.; Moussodia, R.-O.; Bertin, A.; Chen, Y.; Pochan, D. J.; Heiney, P. A.; Klein, M. L.; Percec, V. Self-Assembly of Amphiphilic Janus Dendrimers into Uniform Onion-Like Dendrimersomes with Predictable Size and Number of Bilayers. *Proc. Natl. Acad. Sci. U.S.A.* **2014**, *111*, 9058−9063.
(56) Xiao, Q.; Yadavalli, S. S.; Zhang, S.; Sherman, S. E.; Fiorin, E.; da Silva, L.; Wilson, D. A.; Hammer, D. A.; André, S.; Gabius, H.-J.; Klein, M. L.; Goulian, M.; Percec, V. Bioactive Cell-Like Hybrids Coassembled from (Glyco)Dendrimersomes with Bacterial Membranes. *Proc. Natl. Acad. Sci. U.S.A.* **2016**, *113*, E1134−E1141.
(57) Yadavalli, S. S.; Xiao, Q.; Sherman, S. E.; Hasley, W. D.; Klein, M. L.; Goulian, M.; Percec, V. Bioactive Cell-Like Hybrids from Dendrimersomes with a Human Cell Membrane and Its Components. *Proc. Natl. Acad. Sci. U.S.A.* **2019**, *116*, 744−752.
(58) Xiao, Q.; Sherman, S. E.; Wilner, S. E.; Zhou, X.; Dazen, C.; Baumgart, T.; Reed, E. H.; Hammer, D. A.; Shinoda, W.; Klein, M. L.; Percec, V. Janus Dendrimersomes Coassembled from Fluorinated, Hydrogenated, and Hybrid Janus Dendrimers as Models for Cell Fusion and Fission. *Proc. Natl. Acad. Sci. U.S.A.* **2017**, *114*, E7045−E7053.
(59) Torre, P.; Xiao, Q.; Buzzacchera, I.; Sherman, S. E.; Rahimi, K.; Kostina, N. Y.; Rodriguez-Emmenegger, C.; Möller, M.; Wilson, C. J.; Klein, M. L.; Good, M. C.; Percec, V. Encapsulation of Hydrophobic Components in Dendrimersomes and Decoration of Their Surface with Proteins and Nucleic Acids. *Proc. Natl. Acad. Sci. U.S.A.* **2019**, *116*, 15378−15385.
(60) Li, S.; Xia, B.; Javed, B.; Hasley, W. D.; Melendez-Davila, A.; Liu, M.; Kerzner, M.; Agarwal, S.; Xiao, Q.; Torre, P.; Bermudez, J. G.; Rahimi, K.; Kostina, N. Yu.; Möller, M.; Rodriguez-Emmenegger, C.; Klein, M. L.; Percec, V.; Good, M. C. Direct Visualization of Vesicle Disassembly and Reassembly Using Photocleavable Dendrimers Elucidates Cargo Release Mechanisms. *ACS Nano* **2020**, *14*, 7398−7411.
(61) Kostina, N. Y.; Wagner, A. M.; Haraszti, T.; Rahimi, K.; Xiao, Q.; Klein, M. L.; Percec, V.; Rodriguez-Emmenegger, C. Unraveling Topology-Induced Shape Transformations in Dendrimersomes. *Soft Matter* **2021**, *17*, 254−267.
(62) Kostina, N. Yu.; Rahimi, K.; Xiao, Q.; Haraszti, T.; Dedisch, S.; Spatz, J. P.; Schwaneberg, U.; Klein, M. L.; Percec, V.; Möller, M.; Rodriguez-Emmenegger, C. Membrane-Mimetic Dendrimersomes Engulf Living Bacteria via Endocytosis. *Nano Lett.* **2019**, *19*, 5732−5738.
(63) Buzzacchera, I.; Xiao, Q.; Han, H.; Rahimi, K.; Li, S.; Kostina, N. Y.; Toebes, B. J.; Wilner, S. E.; Möller, M.; Rodriguez-Emmenegger, C.; Baumgart, T.; Wilson, D. A.; Wilson, C. J.; Klein, M. L.; Percec, V. Screening Libraries of Amphiphilic Janus Dendrimers based on Natural Phenolic Acids to Discover Monodisperse Unilamellar Dendrimersomes. *Biomacromolecules* **2019**, *20*, 712−727.
(64) Rosen, B. M.; Wilson, C. J.; Wilson, D. A.; Peterca, M.; Imam, M. R.; Percec, V. Dendron-Mediated Self-Assembly, Disassembly, and Self-Organization of Complex Systems. *Chem. Rev.* **2009**, *109*, 6275−6540.
(65) Sun, H.-J.; Zhang, S.; Percec, V. From Structure to Function via Complex Supramolecular Dendrimer Systems. *Chem. Soc. Rev.* **2015**, *44*, 3900−3923.
(66) Kopitz, J.; Xiao, Q.; Ludwig, A.-K.; Romero, A.; Michalak, M.; Sherman, S. E.; Zhou, X.; Dazen, C.; Vértesy, S.; Kaltner, H.; Klein, M. L.; Gabius, H.-J.; Percec, V. Reaction of a Programmable Glycan Presentation of Glycodendrimersomes and Cells with Engineered


https://doi.org/10.1021/acs.biomac.4c01599
*Biomacromolecules* 2025, 26, 726−737

Human Lectins To Show the Sugar Functionality of the Cell Surface. *Angew. Chem., Int. Ed.* **2017**, *56*, 14677−14681.
(67) Ludwig, A.-K.; Michalak, M.; Xiao, Q.; Gilles, U.; Medrano, F. J.; Ma, H.; FitzGerald, F. G.; Hasley, W. D.; Melendez-Davila, A.; Liu, M.; Rahimi, K.; Kostina, N. Y.; Rodriguez-Emmenegger, C.; Möller, M.; Lindner, I.; Kaltner, H.; Cudic, M.; Reusch, D.; Kopitz, J.; Romero, A.; Oscarson, S.; Klein, M. L.; Gabius, H.-J.; Percec, V. Design−Functionality Relationships for Adhesion/Growth-Regulatory Galectins. *Proc. Natl. Acad. Sci. U.S.A.* **2019**, *116*, 2837−2842.
(68) Percec, V.; Xiao, Q. Helical Self-Organizations and Emerging Functions in Architectures, Biological and Synthetic Macromolecules. *Bull. Chem. Soc. Jpn.* **2021**, *94*, 900−928.
(69) Xiao, Q.; Ludwig, A.-K.; Romanò, C.; Buzzacchera, I.; Sherman, S. E.; Vetro, M.; Vértesy, S.; Kaltner, H.; Reed, E. H.; Möller, M.; Wilson, C. J.; Hammer, D. A.; Oscarson, S.; Klein, M. L.; Gabius, H.-J.; Percec, V. Exploring Functional Pairing between Surface Glycoconjugates and Human Galectins Using Programmable Glycodendrimersomes. *Proc. Natl. Acad. Sci. U.S.A.* **2018**, *115*, E2509−E2518.
(70) Xiao, Q.; Rubien, J. D.; Wang, Z.; Reed, E. H.; Hammer, D. A.; Sahoo, D.; Heiney, P. A.; Yadavalli, S. S.; Goulian, M.; Wilner, S. E.; Baumgart, T.; Vinogradov, S. A.; Klein, M. L.; Percec, V. Self-Sorting and Coassembly of Fluorinated, Hydrogenated, and Hybrid Janus Dendrimers into Dendrimersomes. *J. Am. Chem. Soc.* **2016**, *138*, 12655−12663.
(71) Zhang, S.; Moussodia, R.-O.; Sun, H.-J.; Leowanawat, P.; Muncan, A.; Nusbaum, C. D.; Chelling, K. M.; Heiney, P. A.; Klein, M. L.; André, S.; Roy, R.; Gabius, H.-J.; Percec, V. Mimicking Biological Membranes with Programmable Glycan Ligands Self-Assembled from Amphiphilic Janus Glycodendrimers. *Angew. Chem., Int. Ed.* **2014**, *53*, 10899−10903.
(72) Zhang, S.; Moussodia, R.-O.; Murzeau, C.; Sun, H.-J.; Klein, M. L.; Vértesy, S.; André, S.; Roy, R.; Gabius, H.-J.; Percec, V. Dissecting Molecular Aspects of Cell Interactions Using Glycodendrimersomes with Programmable Glycan Presentation and Engineered Human Lectins. *Angew. Chem., Int. Ed.* **2015**, *54*, 4036−4040.
(73) Zhang, S.; Moussodia, R.-O.; Vértesy, S.; André, S.; Klein, M. L.; Gabius, H.-J.; Percec, V. Unraveling Functional Significance of Natural Variations of a Human Galectin by Glycodendrimersomes with Programmable Glycan Surface. *Proc. Natl. Acad. Sci. U.S.A.* **2015**, *112*, 5585−5590.
(74) Percec, V.; Leowanawat, P.; Sun, H.-J.; Kulikov, O.; Nusbaum, C. D.; Tran, T. M.; Bertin, A.; Wilson, D. A.; Peterca, M.; Zhang, S.; Kamat, N. P.; Vargo, K.; Moock, D.; Johnston, E. D.; Hammer, D. A.; Pochan, D. J.; Chen, Y.; Chabre, Y. M.; Shiao, T. C.; Bergeron-Brlek, M.; Andre, S.; Roy, R.; Gabius, H.-J.; Heiney, P. A. Modular Synthesis of Amphiphilic Janus Glycodendrimers and Their Self-Assembly into Glycodendrimersomes and Other Complex Architectures with Bioactivity to Biomedically Relevant Lectins. *J. Am. Chem. Soc.* **2013**, *135*, 9055−9077.
(75) Zhang, S.; Xiao, Q.; Sherman, S. E.; Muncan, A.; Ramos Vicente, A. D. M.; Wang, Z.; Hammer, D. A.; Williams, D.; Chen, Y.; Pochan, D. J.; Vértesy, S.; André, S.; Klein, M. L.; Gabius, H.-J.; Percec, V. Glycodendrimersomes from Sequence-Defined Janus Glycodendrimers Reveal High Activity and Sensor Capacity for the Agglutination by Natural Variants of Human Lectins. *J. Am. Chem. Soc.* **2015**, *137*, 13334−13344.
(76) Xiao, Q.; Zhang, S.; Wang, Z.; Sherman, S. E.; Moussodia, R.-O.; Peterca, M.; Muncan, A.; Williams, D. R.; Hammer, D. A.; Vértesy, S.; André, S.; Gabius, H.-J.; Klein, M. L.; Percec, V. Onion-like Glycodendrimersomes from Sequence-Defined Janus Glycodendrimers and Influence of Architecture on Reactivity to a Lectin. *Proc. Natl. Acad. Sci. U.S.A.* **2016**, *113*, 1162−1167.
(77) Rodriguez-Emmenegger, C.; Xiao, Q.; Kostina, N. Y.; Sherman, S. E.; Rahimi, K.; Partridge, B. E.; Li, S.; Sahoo, D.; Reveron Perez, A. M.; Buzzacchera, I.; Han, H.; Kerzner, M.; Malhotra, I.; Möller, M.; Wilson, C. J.; Good, M. C.; Goulian, M.; Baumgart, T.; Klein, M. L.; Percec, V. Encoding Biological Recognition in a Bicomponent Cell-Membrane Mimic. *Proc. Natl. Acad. Sci. U.S.A.* **2019**, *116*, 5376−5382.
(78) Xiao, Q.; Delbianco, M.; Sherman, S. E.; Reveron Perez, A. M.; Bharate, P.; Pardo-Vargas, A.; Rodriguez-Emmenegger, C.; Kostina, N. Y.; Rahimi, K.; Söder, D.; Möller, M.; Klein, M. L.; Seeberger, P. H.; Percec, V. Nanovesicles Displaying Functional Linear and Branched Oligomannose Self-Assembled from Sequence-Defined Janus Glycodendrimers. *Proc. Natl. Acad. Sci. U.S.A.* **2020**, *117*, 11931−11939.
(79) Yu Kostina, N.; Söder, D.; Haraszti, T.; Xiao, Q.; Rahimi, K.; Partridge, B. E.; Klein, M. L.; Percec, V.; Rodriguez-Emmenegger, C. Enhanced Concanavalin A Binding to Preorganized Mannose Nanoarrays in Glycodendrimersomes Revealed Multivalent Interactions. *Angew. Chem., Int. Ed.* **2021**, *60*, 8352−8360.
(80) Klajnert-Maculewicz, B.; Janaszewska, A.; Majecka, A. Dendrimersomes: Biomedical Applications. *Chem. Commun.* **2023**, *59* (99), 14611−14625.
(81) Sahoo, D.; Percec, V. From Frank-Kasper, Quasicrystals, and Biological Membrane Mimics to Reprogramming *In Vivo* the Living Factory to Target the Delivery of mRNA with One-Component Amphiphilic Janus Dendrimers. *Biomacromolecules* **2024**, *25*, 1353−1370.
(82) Pardi, N.; Muramatsu, H.; Weissman, D.; Kariko, K. In Vitro Transcription of Long RNA Containing Modified Nucleosides. *Methods Mol. Biol.* **2013**, *969*, 29−42.
(83) Weissman, D.; Pardi, N.; Muramatsu, H.; Karikó, K. HPLC Purification of In Vitro Transcribed Long RNA. *Methods Mol. Biol.* **2013**, *969*, 43−54.
(84) Baiersdörfer, M.; Boros, G.; Muramatsu, H.; Mahiny, A.; Vlatkovic, I.; Sahin, U.; Karikó, K. A Facile Method for the Removal of DsRNA Contaminant from In Vitro-Transcribed mRNA. *Mol. Ther. Nucleic Acids* **2019**, *15*, 26−35.
(85) Nouguier, R. M.; Mchich, M. Alkylation of Pentaerythritol and Trimethylolpropane, Two Very Hydrophilic Polyols, by Phase-Transfer Catalysis. *J. Org. Chem.* **1985**, *50*, 3296−3298.
(86) Nouguier, R.; Mchicj, M. Alkylation of Pentaerythritol by Phase-Transfer Catalysis. 2. Crucial Effect of Aqueous Sodium Hydroxide Solution. *Tetrahedron* **1988**, *44*, 2477−2481.
(87) Nouguier, R. M.; Mchich, M. Alkylation of Pentaerythritol by Phase-Transfer Catalysis. 3. Influence of the Tetrahedral Structure of Pentaerythritol on the Rate and Selectivity of the Phase-Transfer-Catalyzed Reaction. *J. Org. Chem.* **1987**, *52*, 2995−2997.
(88) Dumoulin, F.; Lafont, D.; Huynh, T.-L.; Boullanger, P.; Mackenzie, G.; West, J. J.; Goodby, J. W. Synthesis and Liquid Crystalline Properties of Mono-Di and Tri-O-alkyl Pentaerythritol Derivatives Bearing Tri-Di- or Monogalactosyl Heads: The Effects of Curvature of Molecular Packing on Mesophase Formation. *Chem.—Eur. J.* **2007**, *13*, 5585−5600.
(89) May, J. P.; Undzys, E.; Roy, A.; Li, S.-D. Synthesis of a Gemcitabine Prodrug for Remote Loading into Liposomes and Improved Therapeutic Effect. *Bioconjugate Chem.* **2016**, *27*, 226−237.
(90) Steglich, W.; Höfle, G. N. *N* -Dimethyl-4-pyridinamine, a Very Effective Acylation Catalyst. *Angew. Chem., Int. Ed. Engl.* **1969**, *8*, 981.
(91) Neises, B.; Steglich, W. Simple Method for the Esterification of Carboxylic Acids. *Angew. Chem., Int. Ed.* **1978**, *17*, 522−524.
(92) Höfle, G.; Steglich, W.; Vorbrüggen, H. 4-Dialkylaminopyridines as Highly Active Acylation Catalysts. [New Synthetic Method (25)]. *Angew. Chem., Int. Ed. Engl.* **1978**, *17*, 569−583.
(93) Jiang, X.; Fleischmann, S.; Nguyen, N. H.; Rosen, B. M.; Percec, V. Cooperative and Synergistic Solvent Effects in SET-LRP of MA. *J. Polym. Sci., Part A: Polym. Chem.* **2009**, *47*, 5591−5605.
(94) Zhang, X.; Su, K.; Wu, S.; Lin, L.; He, S.; Yan, X.; Shi, L.; Liu, S. One-Component Cationic Lipids for Systemic mRNA Delivery to Splenic T Cells. *Angew. Chem., Int. Ed.* **2024**, *63*, No. e202405444.


https://doi.org/10.1021/acs.biomac.4c01599
*Biomacromolecules* 2025, 26, 726−737